Syracuse University

SURFACE

Theses - ALL

6-2014

Assessing landfill contamination in Wyoming

Maxwell Blaine Gade
Syracuse University

Follow this and additional works at: https://surface.syr.edu/thesis

Recommended Citation

Gade, Maxwell Blaine, "Assessing landfill contamination in Wyoming" (2014). *Theses - ALL*. 23.
https://surface.syr.edu/thesis/23

This Thesis is brought to you for free and open access by SURFACE. It has been accepted for inclusion in Theses - ALL by an authorized administrator of SURFACE. For more information, please contact surface@syr.edu.

Abstract

The Wyoming Department of Environmental Quality (WDEQ) suggested landfills across the State are contaminating groundwater with landfill leachate, soliciting an investigation of what useful aquifers might be contaminated, and whether remediation could be appropriate. My research goal is to broadly characterize groundwaters statewide to analyze the validity of WDEQ contamination claims, discuss the reliability of the WDEQ determination, and provide a feasible model of natural groundwater conditions. Volatile anthropogenic compounds such as acetone, methyl chloride, and dichlorobenzene are present in landfill leachte in discarded solvents and clearly can be used to characterize landfill leachate contamination. However, the WDEQ also uses concentrations of inorganic solutes, such as bicarbonate, sulfate, and chloride to fingerprint landfill contamination of groundwater. I explored an extensive chemical database on groundwater quality around landfills across Wyoming and found that typical solute concentrations of sodium, sulfate, and chloride the State uses to indicate contamination do not significantly correlate with volatile anthropogenic organics in contaminated water samples, such as benzene and toluene. Furthermore, correlations between major ions in the WDEQ dataset reflect naturally poor water quality where concentrations of chloride, iron, magnesium, sodium and sulfate exceed regulatory standards because of natural processes including ion exchange and evaporation. In addition, concentrations of the minor solutes iron and manganese commonly exceeded thermodynamic constraints by orders of magnitude because particulate material in samples was not removed prior to analysis. To determine how poor water quality naturally evolves in Wyoming basin fill and to determine the extent to which sampled water beneath landfills may be recently recharged I focused on the Sand Draw landfill, for which filtered hydrologic and geochemical data were available. Carbon isotopes of dissolved organic carbon

and water isotopic data collected at the Sand Draw landfill indicate that water under this landfill occurs not in a regional water table but in perched water zones so isolated from modern recharge that the water is thousands of years old. I used Netpath, an interactive code for modeling net geochemical reactions developed by the USGS, to develop a feasible geochemical model representing the source of naturally poor water quality in the absence of landfill leachate contamination at the Sand Draw landfill. These heuristic simulations indicate ion exchange coupled to carbonate dissolution lead to poor drinking water quality in the basins of Wyoming.

Assessing landfill contamination in Wyoming

by:

Maxwell B. Gade

B.S., University of Nebraska, Lincoln, NE, 2012

MASTERS THESIS

Submitted in partial fulfillment of the requirements for the degree of

Master of Science in Earth Sciences

Syracuse University

June 2014

Copyright © Maxwell B. Gade 2014

All rights reserved

Acknowledgements

I would like to acknowledge the guidance, patience, and enthusiasm of my advisor, Dr. Don Siegel, who presented me with a challenging new subject and a large dataset, both which I was unknowingly unprepared for, and allowed me to make the necessary mistakes to build a base on which my future expertise is developing. I thank my entire committee; including Dr. Laura Lautz, Dr. Zunli Lu, and Dr. Scott Samson, for having the patience to accept a barrage of questions from me without notice throughout the semesters. I thank Dr. Lautz for her support and inclusion while I completed my thesis and was simultaneously given leadership opportunities with Project SWIFT. I thank Dr. Lu for his interest in my work which spurred a broader analysis of the geochemical patterns in my dataset. I thank Dr. Samson for continually challenging me to have a deeper understanding of geochemical and isotopic processes. I also thank the faculty, staff, and fellow students in the department for being supportive of my academic work and matching my enthusiasm for the department. Finally, I thank my family for their undying support throughout my academic career.

Table of Contents

Abstract—i

Title Page—iii

Copyright Notice—iv

Acknowledgements—v

Table of Contents—vi

List of Figures—vii

List of Tables—viii

Introduction—1

- Landfill Processes—5

Site Description—7

- Geology and Hydrology of Wyoming—7
- Geology and Hydrology of the Wind River Basin—13
- Geology and Hydrology of the Sand Draw Landfill—14

Methods—15

- Geochemical Patterns—15
- Isotopes of Groundwater—16
- Isotopes of Carbon—17
- Tritium Dating—20
- Geochemical Modeling—21
- Model Input Significance Testing—25

Results and Discussion—26

- Statewide Geochemical Patterns in Landfills—26
- Geochemical Modeling—32

Conclusions—35

Future Work and Recommendations—36

Appendices—38

References—46

Vita—53

List of Figures

Figure 1: Map of Wyoming——3

Figure 2: Leachate Plume——5

Figure 3: Leachate Geochemical Profiles——6

Figure 4: Map of Wyoming Mountain Ranges and Basins——7

Figure 5: Wyoming Stratigraphy——9

Figure 6: Map of the Sand Draw Landfill——25

Figure 7: Graphs of Basin Geochemistry——26

Figure 8: Basin Hydrochemical Facies——27

Figure 9: Contamination Status Hydrochemical Facies——27

Figure 10: Graphs of TOC and Ammonia v. Chloride by Contamination Status——28

Figure 11: Graphs of TOC and Chloride v. Total VOCs——29

Figure 12: Graphs of TOC and Ammonia v. Chloride by Landfill Type——29

Figure 13: Geochemical Patterns——30

Figure 14: Iron and Manganese Thermodynamic Exceedances——31

Figure 15: Deuterium and Oxygen Isotopes from the Sand Draw Landfill——33

Figure 16: Model Input Significance Testing Results——34

List of Tables

Table 1: Landfill Chemical Reactions——6

Table 2: Stoichiometric Coefficients of Modeled Phases——22

Table 3: Sand Draw Landfill Dataset——23

Table 4: Basic Reactions Involving Organic Carbon——23

Table 5: Water Quality Standards and Exceedances——26

Table 6: Observed and Computed Groundwater Ages——33

Introduction

In the past, landfills in Wyoming and elsewhere in the arid American west have been built without protective engineered liners because regulatory agencies believed the aridity of the climate was sufficient to prevent leachate formation and infiltration. However, recently the Wyoming Department of Environmental Quality (WDEQ) suggested broad contamination of groundwater by landfill leachate and the need for hundreds of millions of dollars of potential remediation at the expense of counties and landfill owners. The cost obligation to local governments is approximately $164 million and the estimated statewide cost is $226 million, over 20 years. Thousands of groundwater samples from 521 monitoring wells installed around landfills since 2006 provided Wyoming a statewide, 363,000 data point dataset of groundwater quality from which they based their conclusions (WDEQ, 2010).

The WDEQ considered that groundwater had been impacted by landfills when constituents commonly associated with landfill leachate (e.g. pH, Total Dissolved Solids, Bicarbonate, Sulfate, Chloride, Ammonia and Volatile Organic Compounds) increased in concentration down-gradient of landfills to above EPA maximum contaminant levels (MCLs) or DEQ-established Groundwater Protection Standards (GPSs).

An MCL is “the level of a contaminant in drinking water below which there is no known or expected risk to health” (EPA, 2009). Groundwater Protection Standards (GPSs) were health-based concentration levels meeting WDEQ Water Quality Rules and Regulations requirements (2007). Based on MCL exceedances the Wyoming Department of Environmental Quality is determining whether landfills need to be relined or capped, to control precipitation percolating through waste, and if groundwater remediation may be necessary (WDEQ, 2010).

The WDEQ sampled groundwater at landfills from on-site monitoring wells. The monitoring well to be sampled was bailed for 3 well volumes or until the well was bailed dry. After the well had been bailed groundwater samples were collected for analysis. Samples were taken from the center of the water column. If bailed water was silty it was left to settle before samples were collected. Specific conductance, hardness (as $CaCO_3$), pH, and turbidity were determined in the field. Samples were then stored on ice. If a disposable bailer was not used it was decontaminated prior to sample collection unless sampling occurred immediately after bailing. After sampling non-disposable bailers were decontaminated using detergent and hot tap water, a tap water rinse, and two distilled water rinses (WDEQ, 1995).

Samples taken for inorganic analyses were first processed using acid digestion for total recoverable and dissolved metals analyses. Microwave assisted acid digestion was sometimes used for sediments, sludges, soils, oils, and siliceous and organically based matrices. Inorganic analytes were generally determined by Inductively Coupled Plasma Mass Spectrometry (ICP-MS) or Inductively Coupled Plasma Atomic Emission Spectrometry (ICP-AES). Volatile and semivolatile organics are analyzed by gas chromatography and mass spectrometry combined with vacuum distillation and cryogenic trapping or thermal extraction for soil and sludge samples (EPA, 2007).

The large dataset of water quality tests at landfills from the 2010 WDEQ report includes multiple years of groundwater sampling from wells at 134 landfills (see map Figure 1). However, a question remains whether water quality in violation of exceedances standards may be due to natural versus anthropogenic factors. For example, the aridity of the western United States causes evapoconcentration of natural solutes in shallow aquifers, resulting in naturally high solute concentrations due to the high solubility of base-cation evaporites common in arid and

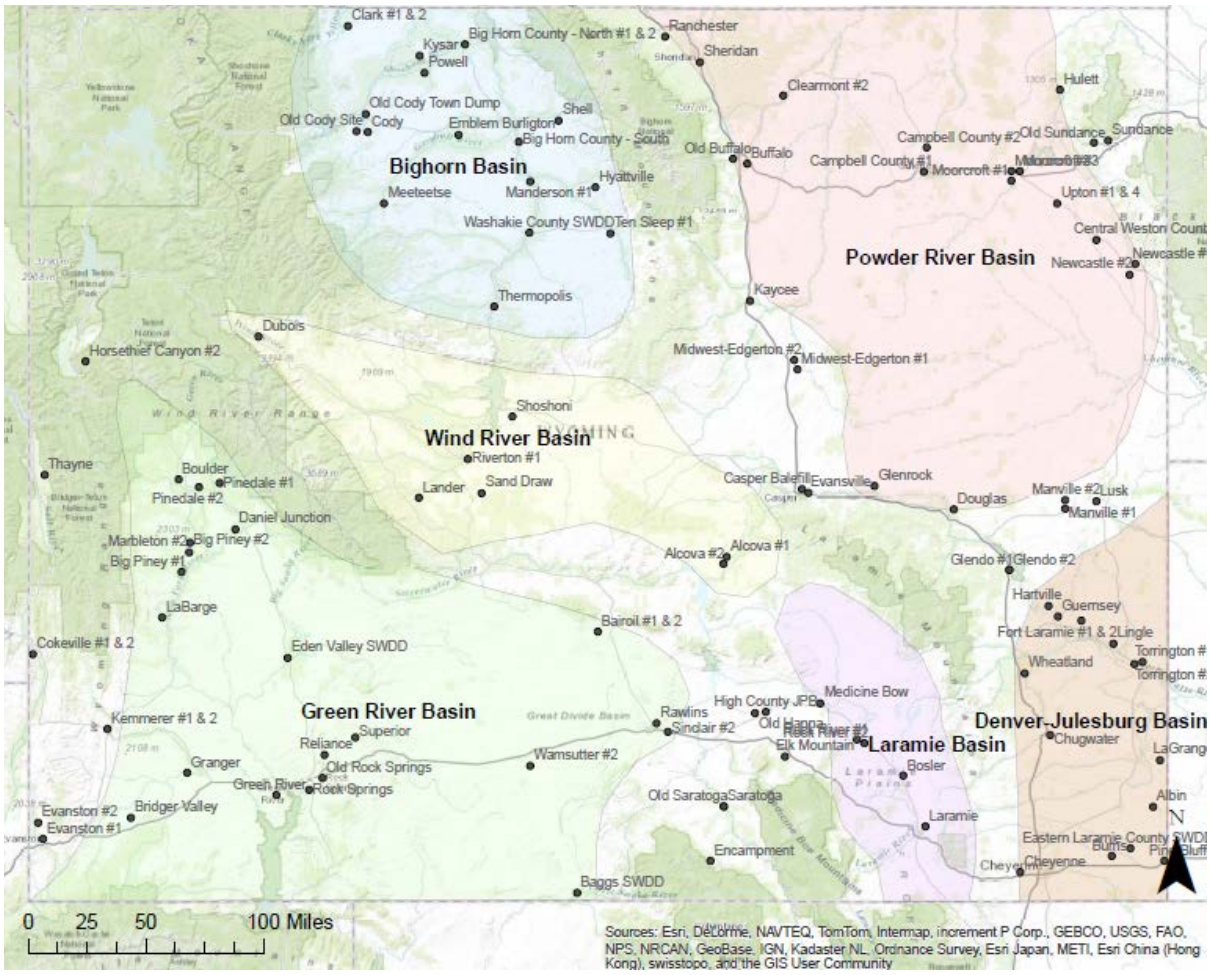

Figure 1: An initial analyses of landfill water quality data was done on a large scale to see if geochemical patterns existed basin-wide. This map shows the locations of basins and landfills across Wyoming.

semi-arid environments (Nativ et al., 1997; Hidalgo and Cruz-Sanjulián, 2001), coupled with evaporation from the water table (Ong et al., 1995, Gurdak and Roe, 2010). According to WDEQ rules and regulations solid waste water samples are not filtered prior to laboratory analysis so groundwater samples accureately represent natural groundwater quality. If water samples are not filtered before analysis, particulates included in sampling, from local siltstone and claystone can lead to erroneous high concentrations of dissolved metals in samples (WDEQ, 2013; Saar, 1997; Gibb et al., 1981). These complications cause “false positives” or regulatory assumption of contamination from landfill leachate in places where water quality is naturally poor or because of improper sampling. These problems together make landfill water contamination in the arid west

more difficult to identify than in water rich eastern States, and therefore require different diagnostic chemical tools.

Here, I focused on evaluating the quality of the WDEQ dataset and sampling protocols, and then related observed concentrations to fundamental thermodynamic controls over maximum plausible solute concentrations that can occur in solution for those solutes considered to be potential indicators of landfill leachate contamination.

I also present a more detailed analysis of the Sand Draw landfill in the Wind River Basin where I used filtered geochemical data, including isotopic measurements, to explore whether observed geochemistry could be explained by natural processes impacting water quality, rather than exclusively by landfill leachate contamination. To this end, I incorporated mass-balance and forward reaction geochemical modeling to constrain natural evolution of water quality in the Wind River basin shallow formation that may be affected by landfill leachate. These results will enable the WDEQ and others to develop more robust methods to determine the degree to which contamination actually occurs under existing landfills or is merely perceived to occur because concentrations of solutes in groundwater exceed drinking water standards.

I hypothesize that 1) the common indicators of leachate-groundwater interaction cannot be used to determine contamination at arid-environment landfills, 2) the sampling protocols of the WDEQ are faulty and results in falsely characterizing landfill water chemistry where contamination appears to have occurred, and 3) the hydrology and geochemistry of arid-environment landfills generally precludes contamination by landfill leachate except in unusual hydrogeologic cases.

Landfill Processes

When precipitation percolates through municipal landfill waste, bacterial and fungally-driven waste decomposition forms leachate which migrates downward to the water table from which a contaminant plume evolves below the landfill. Most degradation of waste consists of cellulose oxidation, which in the process, consumes oxygen and creates anoxic conditions within the landfill and in leachate produced from it. A sequence of oxidation-reduction reactions occurs as leachate forms and is transported beneath the landfill with groundwater: oxidation, denitrification, iron and manganese reduction, sulfate reduction, and methanogenesis. This process consumes oxygen, causing anoxic conditions and commonly produces leachate plumes of dissolved ammonium, iron, manganese, and chloride (Figure 2) (Baedecker and Back, 1979; Christensen et al. 2001).

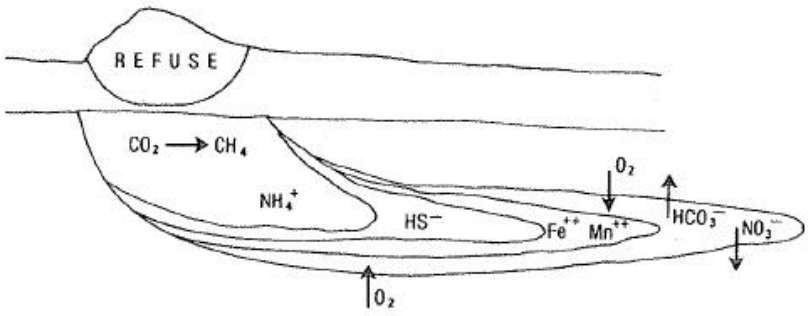

Figure 2: Late stage chemical evolution of a hypothetical redox zone near a landfill (Baedecker and Back, 1979)

In addition, construction debris can dissolve, releasing sulfate (e.g. from sheet rock) and if landfilled waste is covered by clayey soils to prevent waste dispersal, ion-exchange processes can reduce base cation hardness. Chloride concentrations from organic matter in waste also usually are elevated. The sum of all these processes outlined in Table 1 lead to leachate typically of a Na-SO_4-Cl type with high concentrations of iron, manganese, ammonium and dissolved organic carbon.

Municipal waste landfills also commonly have leachate with anthropogenically derived volatile organic solvents and hydrocarbons (VOCs), such as trichloroethene and benzene,

respectively. These compounds derive from household cleaning agents to disposed paints and construction material. Anthropogenically derived VOCs are even more common in industrial waste landfills and sometimes in landfills designed to only accept construction debris (EPA, 2012).

Typical Chemical Reactions Associated with Municipal Waste Landfills	
Oxidation	$2O_2(g) + 2H^+ = 2H_2O$
Denitrification	$NO_3^- + H^+ = N_2(g) + H_2O$
Iron Reduction	$FeOOH(s) + HCO_3^- + 2H^+ = FeCO_3(s) + 2H_2O$
Manganese Reduction	$MnO_2(s) + HCO_3^- + 3H^+ = MnCO_3(s) + H_2O$
Sulfate Reduction	$SO_4^{2-} + 9H^+ = HS^- + 4H_2O$
Methanogenesis	$CH_3COOH = CH_4 + CO_2$ or $CO_2 + 8H^+ = CH_4(g) + 2H_2O$

Table 1: The typical chemical reactions associated with municipal waste landfills are oxidation, denitrification, iron and manganese reduction, sulfate reduction, and methanogenesis (Christensen et al. 2001).

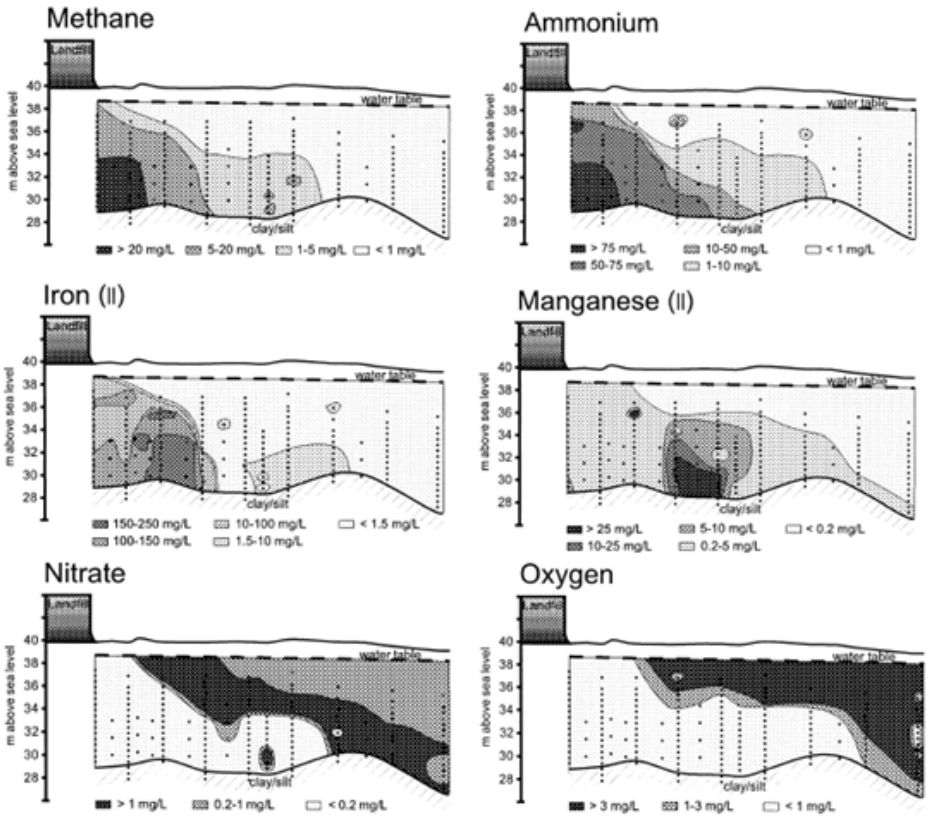

Figure 3: Geochemical profiles of methanogenesis, reduction, denitrification, and oxidation at a contaminated landfill show the chemistry of landfill leachate. The reduction and oxidation reactions that occur as landfill leachate reacts with the atmosphere and surrounding geology provides common chemical indicators used to identify landfill leachate contamination (From Christensen et al., 2001).

The aridity of Wyoming and other western States leads to less leachate production than produced under landfills in wetter eastern States, and Wyoming landfills have a lower mass flux of leachate. An example of the chemistry of groundwater indisputably contaminated by landfill leachate is shown in Figure 3 (After Christensen et al., 2001) showing geochemical profiles dominated by methanogenesis (methane), reduction (ammonium, iron, and manganese), denitrification (nitrate) and oxidation (oxygen).

Site Description

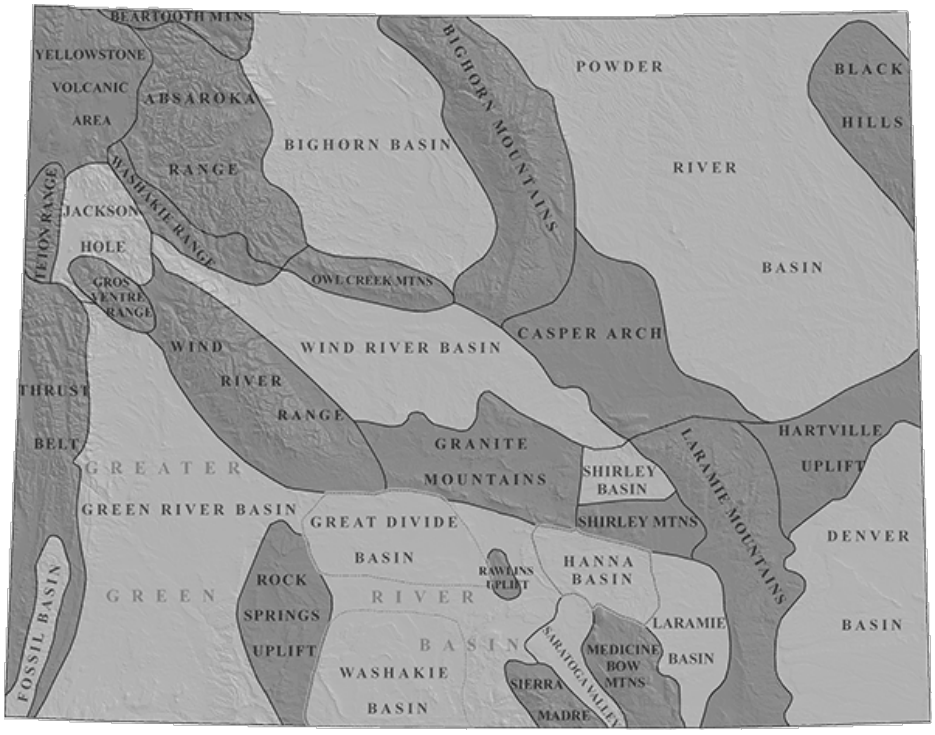

Figure 4: Map of Wyoming mountain ranges and basins (WSGS, 2014).

Geology and Hydrology of Wyoming

Landfills in Wyoming have been constructed mostly on intermountain basin fill. Early in its geologic history, from the Paleozoic to early Mesozoic eras, marine deposits of limestone, dolostone, shale, siltstone, and sandstone were deposited over much of Wyoming in the western interior seaway. During the Cretaceous, alluvium was deposited across Wyoming. During the

Laramide orogeny from late Cretaceous to late Eocene time, subduction of a western crustal plate below the North American plate uplifted mountain ranges in western Wyoming and intervened the Big Horn, Powder River, Green River, Laramie, Denver, and Wind River basins (Figure 4). These basins are filled with Cretaceous and Tertiary-age sediment derived from eroding bedrock on the basin flanks. Basin sedimentary deposits are between 1,000 and 6,000 m thick, but constitute a fraction of sediments from uplift erosion during the Laramide orogeny. The majority of Laramide sediment deposits were transported by large rivers to the Gulf of Mexico (Miller et al., 1992).

The Bighorn and Powder River Basin interiors consist of thick, flat-lying Eocene and Paleocene rocks surrounded by Mesozoic rocks dipping into the basins. The Mesozoic and Paleozoic rocks are folded into anticlines and synclines which contain oil and gas resources. The western edge of the Bighorn basin is defined by the volcanic Absaroka Range, and to the east the Bighorn and Powder River basins are separated by the Bighorn Mountains, which has an Archean granitic and metamorphic core. The Powder River Basin is defined by the Black Hills uplift to the east, and the Casper Arch and Hartville Uplift to the south (Love et al. 1978a, 1987b, 1979a, 1979b, 1980, 1990; Pierce, 1978; Gill and Cobban, 1973; Keefer, 1972; Robinson et al. 1964).

The Wind River Basin contains thick Upper Cretaceous and lower Tertiary sedimentary rocks which contain important coal, oil, and natural gas reserves. The Wind River Basin is separated from the Bighorn Basin by the Owl Creek Mountains to the north, separated from the Green River Basin by the Wind River Range to the west, and is bound in the east and south by the Casper Arch and the appropriately named Granite Mountains. The Green River Basin is bordered in the west by the Wyoming Thrust Belt, by the Wind River Range in the north, and is

composed of a complex of basins extending to the east separated by the Rock Springs uplift including the Green River, Washakie, and Great Divide basins. The Green River Basin is separated from the eastern Laramie and Denver basins by the Sierra Madre Mountains (Roehler, 1991; Oriel and Platt, 1980; Love et al. 1979a; Denson and Pipiringos, 1974; Keefer, 1965, 1970, 1972; Keefer and Van Lieu, 1966; Bradley, 1954).

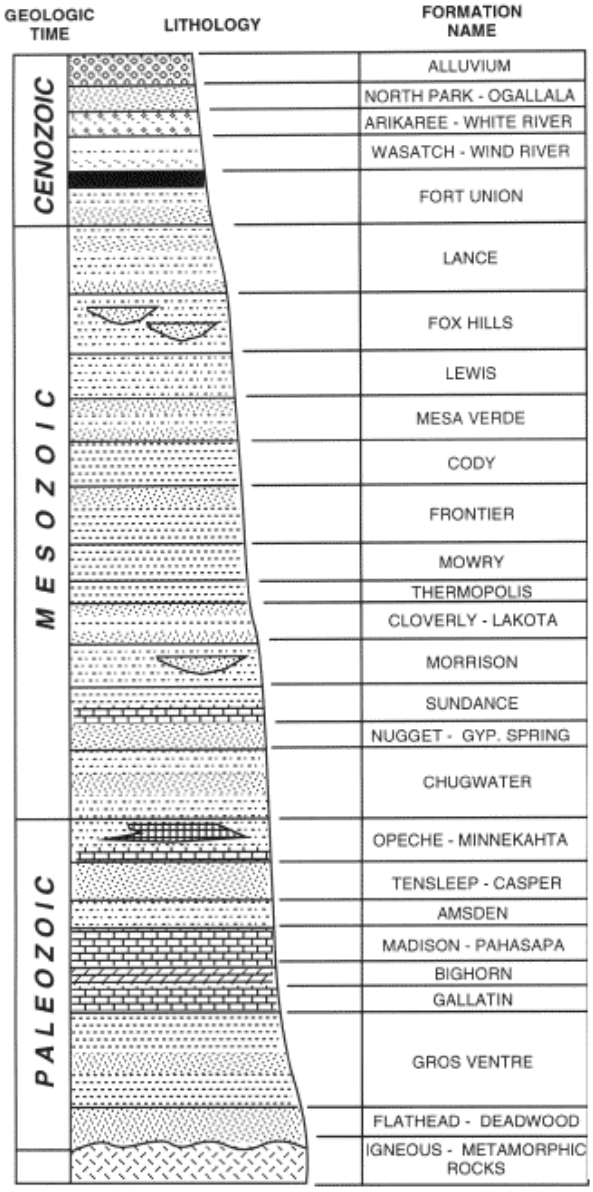

Figure 5: Generalized Stratigraphy of Wyoming (modified after WWPSC, 1997 – Figure E-2)

The Laramie and Denver basins are separated by the Laramie Mountains. The Laramie Basin contains thick Upper Cretaceous and Tertiary clastic sedimentary sequences derived from adjacent uplands which contain thick coal seams. The Denver Basin contains horizontal Later Tertiary age strata unconformably above a large downfolded trough composed of Paleozoic and Mesozoic age rocks extending into northeastern Colorado (Love et al. 1980, 1979a; Gill and Cobban, 1973; Gill et al. 1970; Maughan, 1964; McGrew, 1963).

A generalized stratigraphic column of geologic formations across Wyoming (Figure 5) shows the major water-bearing units across the state: the North Park-Ogallala, Arikaree-White River, Wasatch-Wind River, Fort Union,

Mesaverde, Cloverly-Lakota, Nugget-Gypsum Spring, Tensleep-Casper, Madison-Pahasapa, Bighorn, and Flathead-Deadwood aquifer systems. The Lance, Fox Hills, Sundance, and Phorphoria (not pictured) Formations and unconsolidated Quaternary alluvium also contain groundwater (Feathers et al. 1980; Libra et al. 1981a, 1981b; Richter, 1981a, 1981b; Ahern et al. 1981; Collentine et al. 1981).

Alluvium is composed of silt, sand, and gravel in basin flood plains, fans, terraces, and slopes deposited throughout the Quaternary and derived from exposed and eroded formations. Fan deposits are generally locally derived clasts and tertiary gravels, with some glacial deposits on the east slope of the Wind River Range.

The North Park-Ogallala system is part of the High Plains aquifer system, is located in the Denver Basin, and is primarily sandstone with claystone, conglomerate, siltstone and limestone. The Arikaree Formation is primarily sandstone and contains layers of ash while the White River Formation is primarily fine-grained mixed clastic sedimentary rocks and includes mudstone, tuffaceous claystone, and volcanic rocks and ash from the Absaroka volcanic field. The Wasatch-Wind River system is primarily mudstone and claystone. The Wasatch Formation also contains carbonaceous shale and arkosic sandstone and the Wind River Formation includes lenticular coal and conglomerate units. The Fort Union Formation is primarily sandstone but also contains shale and coal beds that thin across the State from east to west.

The Lance Formation is primarily sandstone with green shale and conglomerate lenses in north Wyoming and thin coal and carbonaceous shale beds in south and northeastern Wyoming. The Fox Hills Formation is sandstone and shale containing marine fossils above Lewis Formation marine shale. The Mesaverde Formation in north Wyoming consists of sandstone, gray sandy shale, and coal beds and in the Powder River Basin it is solely Parkman Sandstone. In

south Wyoming the Mesaverde Group consists of Almond Formation sandstone and carbonaceous shale, Ericson Sandstone, and the Rock Springs and Blair Formations at the Rock Springs uplift. The Mesaverde Group in the Laramie Basin consists of Pine Ridge Sandstone and the Rock River Formations which are both sandstone and contain thin coal beds and sandy shale respectively.

The Frontier Formation sandstone and Cody, Mowry and Thermopolis shales were deposited in the western interior seaway during the Cretaceous. The Cody Formation consists of shale and siltstone in the Yellowstone area and shale and siltstone with fine-grained sandstone elsewhere. The Frontier Formation is light sandstone and dark shale and in the Wyoming Thrust Belt includes oyster coquina in the upper part and coal and lignite in the lower part of the formation. The Mowry Formation is hard siliceous shale containing fish fossils and bentonite beds and the Thermopolis Formation is soft black fissle shale.

The Cloverly-Lakota system is composed of the Cloverly Formation and the Lakota Formation, which is part of the Inyan Kara Group. The Cloverly, Morrison, Sundance, Nugget, Gypsum Spring, and Chugwater Formations were similarly deposited in the Triassic, Jurassic, and Early Cretaceous. The Cloverly Formation consists of rusty to light-gray sandstone, lenticular chert-pebble conglomerate, and bentonic claystone. The Lakota Formation is sandstone with sandstone conglomerate and sandy claystone (Mapel and Pillmore, 1963). The Morrison Formation is composed of siliceous claystone with limestone nodules and silty sandstone. The Sundance Formation is green-gray glauconitic sandstone and shale underlain by red and gray nonglauconitic sandstone and shale. The Nugget Formation is red crossbedded quartz sandstone. The Gypsum Spring Formation consists of interbedded red shale, dolomite, and gypsum. Groundwater from the Sundance Formation in the Green River, Washakie, and Great Divide

Basins and at the Rock Springs uplift have been found to be saline and briny with State agricultural- and livestock-use standard exceedances of chloride, iron, sulfate, and TDS (Clarey et al., 2010).

The Chugwater Formation is red siltstone and shale with thin gypsum near the base of the formation. In north Wyoming the upper middle Chugwater Formation contains the 5-10 foot thick Alcova limestone. The Permian age Phosphoria Formation below that is a lesser carbonate water-bearing unit below the Wind River Basin consisting of chert, sandstone, limestone, quartzite, and a shale with phosphorite base. The Opeche shale and Minnekahta limestone are the basal formations of the Phosphoria Group of northeastern Wyoming (Sheldon, 1923).

The Casper Formation contains thick red sandstone beds underlain by pink and gray limestone. The Tensleep Sandstone contains thin limestone and dolomite beds and the Amsden Formation contains red and green shale and dolomite. The topmost beds of Tensleep Sandstone contain Permian fossils in the Washakie Range, Owl Creek Mountains, and southern Bighorn Mountains. The Madison (Pahasapa) Group consists of Mission Canyon Formation limestone and dolomite, underlain by cherty Lodgepole Formation limestone and dolomite.

Below the Madison Group lies siliceous Bighorn Dolomite in the northern Yellowstone area, and the Thrust belt and northern Wyoming, where it is cliff forming and locally dolomitic limestone. The Cambrian Gallatin Formation limestone is mottled, dense, and lies above the Gros Ventre Formation; dense limestone sandwiched between layers of soft green micaceous shale. The Flathead and Deadwood Formations are red and brown quartzitic sandstone above lower Cambrian limestone and qlauconitic quartzitic sandstone. There are Archean plutonic rocks in the Wind River Range, granite gneiss containing diorite and quartz diorite facies, and the Bighorn Mountains, containing quartz diorite and quartz monazite facies. Archean age

layered granitic gneiss in the Bighorn Mountains metamorphosed 3,000 Ma (Love and Christensen, 1985).

Geology and Hydrology of the Wind River Basin

The Wind River Basin of southwestern Wyoming began forming as it down-warped from the late Cretaceous to the Eocene, accompanied by the Wind River Range and the Bridger and Owl Creek Mountains uplifting along reverse faults surrounding the basin. The uplifted mountains eroded and sediment was deposited over Eocene sediments already filling the basin, until early Pliocene. From the middle to late Pliocene the Wind River Basin and surrounding mountains were further uplifted and sediment deposited before the late Eocene eroded away. Precambrian granite, granite gneiss, and schist mountain ranges refilled the basin with Eocene and later marine sediments and alluvium (Keefer, 1970).

The valley fill of the Wind River Basin consists of the Split Rock and Wind River formations containing shallow perched lenticular sandstone aquifers confined by units of clayey mudstone. The basin receives relatively low precipitation, 15 – 25 centimeters annually. Recharge to Quaternary and Tertiary aquifers in the basin ranges from less than 3 centimeters in the basin interior to 25 centimeters annually next to mountains and through alluvial fans, from combined precipitation, recharge from Wind River Range snowmelt, and basin drainage to the Wind and Popo Agie Rivers. Below alluvial aquifers in the Wind River Basin major regional aquifers include the sandstone Split Rock (Arikaree), Wind River, and Fort Union-Lance aquifers which are confined from below by the Indian Meadows claystone, Meeteetse-Lewis shale confining unit, and the Cody Formation shale, respectively (Taucher et al., 2012).

The alluvial aquifers of the Wind River Basin consist of lenticular sandstone in Quaternary unconsolidated alluvium 50 to 200 feet thick. Alluvium is composed of sandstone,

limestone, dolomite, and gypsum sediments derived from the erosion of the Cloverly, Morrison, Sundance, Nugget, Gypsum Spring, and Chugwater Formations. Alluvium aquifers exceeded EPA Secondary MCLs of TDS, sulfate, manganese, iron, and chloride. The thickness of the Split Rock Formation that composes the Split Rock aquifer ranges between 0 and 930 feet. The Wind River Formation that composes the Wind River aquifer is between 100 and 5,000 feet thick from mountain range to basin axis. The depth to high yield aquifers with high water quality is hundreds of feet deep and the reliance of the town of Riverton, at the center of the Wind River Basin and north of the Sand Draw landfill, on the Wind River aquifer has caused water levels in area wells to be lowered by approximately 30 feet (Taucher et al. 2012).

Geology and Hydrology of the Sand Draw Landfill

The Sand Draw landfill is underlain by surficial Quaternary and Tertiary fluvial siltstone, claystone, shale and alluvium (Green and Drouillard, 1994). The landfill was placed on a shallow groundwater divide, a recharge area, next to Beaver Creek, a tributary to the Little Wind River. Groundwater flowing below the Sand Draw landfill flows northwest, towards Beaver Creek, and southeast of the landfill. All water infiltrating at the Sand Draw landfill eventually flows to the Wind River (Taucher at al. 2012).

From a past consulting analysis by Siegel (2011, unpublished) it was found that water levels measured in monitoring wells in a westward planned expansion at the Sand Draw landfill do not apparently reflect the regional water table elevation, but may reflect compartmentalization of perched water in isolated permeable units within clayey sediments. Head levels in the center of the landfill are higher than on the perimeter, where head levels are hundreds of feet above the approximate regional water table. Unchanging water levels over the last ten years also imply compartmentalization, with subtle changes in water levels related to atmospheric pressure and

not recharge or evaporation. A resistivity survey showed an apparent stratigraphic section, notably silty and clayey, with no continuous saturated zone within the upper 150 feet of sediment and strong evidence that water levels are from perched water zones.

In a study of the Lower Eocene Willwood Formation, equivalent to the Wind River Formation, in the Bighorn Basin, Neasham and Vondra (1972) noted a predominance of limestone and dolomite cobbles in conglomerates and argillaceous arkose cemented with calcite, silica and iron oxide. Potassium feldspars are more abundant than plagioclase, and the clay mineralogy of Willwood mudstones is primarily montmorillonite, illite and clay mica. In another study of the sedimentology and geochemistry of the lower Eocene strata in the Wind River Basin, Fan and others (2011) found that Wind River Formation lithic grains were less than 5 percent volcanic, dominated by micritic carbonate, and included phyllite, siltstone, and quartzite derived from sedimentary and metasedimentary strata. Samples consisted mostly of monocrystalline quartz, feldspar, and lithic grains with average modal compositions of lithic arkose (Qm:F:Lt = 41:26:33) and subarkose (Qt:F:L = 56:26:18). The feldspar K/P ratio varied between 0.6 and 4.7. Eocene sandstones were primarily cemented by calcite. Knowing this mineralogy constrains the plausible water rock interactions that naturally occur in the Wind River Basin and which might be modified by contamination by landfill leachate.

Methods

Geochemical Patterns

For each reported groundwater analysis from monitoring wells around landfills in the Wind River Basin, I used Piper diagrams to compare the hydrochemical facies of WDEQ groundwater samples that did or did not have VOC contamination, were in different basins

across the state, and received different types of waste. A Piper diagram classifies hydrochemical facies of water in terms of major-ion percentages (Freeze and Cherry, 1979).

I also applied bivariate analyses comparing landfills statewide that were identified as contaminated or uncontaminated. I also compared landfills receiving different waste (municipal solid waste, industrial waste, and construction waste) and the presence of organic contaminants in each type of landfill. Bivariate comparisons can be used to compare and contrast groups of samples and are useful in illustrating geochemical trends in a dataset. Comparing sample chemistry to expected stoichiometric relationships between two solutes provides a visual and quantitative representation of the geochemistry. The use of bivariate quantitative analyses to characterize groundwater is common; for examples see Freeze and Cherry (1979) and Appelo and Postma (1993).

Isotopes of Groundwater

A water molecule is composed of two hydrogen atoms and an oxygen atom. Hydrogen has two naturally occurring stable isotopes: ^{1}H and ^{2}H (deuterium). Oxygen has three naturally occurring stable isotopes: ^{16}O, ^{17}O, and ^{18}O. The hydrogen atoms of a water molecule can either be ^{1}H or ^{2}H and the oxygen atom can be ^{16}O, ^{17}O, or ^{18}O. The isotope ratios (*R*) or the different isotopes of a water molecule, $^{18}O/^{16}O$ and $^{2}H/^{1}H$, are expressed in delta units (δ) measured as per mil (parts per thousand or ‰) relative to standard mean ocean water (SMOW) (Equation 1). The ratios of hydrogen and oxygen isotopes in water are expressed as $\delta^{2}H$ and $\delta^{18}O$ respectively. During the global cycling of water by evaporation and precipitation, the heavier isotopes of hydrogen (^{2}H) and oxygen (^{18}O) in water are preferentially precipitated and lighter isotopes (^{1}H and ^{16}O) are preferentially evaporated, a process called isotope fractionation. When you plot ratios of the hydrogen isotopes against the ratios of the oxygen isotopes in rain and snow, they

fall on a straight line, called the "Local Meteoric Water Line" ("Water Line" in this report) unique for each climatic and topographic region, but fairly close to that for all global precipitation (Freeze and Cherry, 1979; Clark and Fritz, 1997).

$$\delta‰ = [(R - R_{standard})/R_{standard}] \times 1000 \quad (1)$$

The isotopic values of $\delta^{18}O$ (oxygen) and $\delta^{2}H$ (deuterium) change regionally, over time, at different latitudes and temperatures, and can change as a result of evaporation, condensation, freezing, and melting (Freeze and Cherry, 1979). The general relationship between $\delta^{18}O$ and $\delta^{2}H$ in water that has not undergone secondary isotopic fractionation is defined by Equation 2, the global meteoric water line (Craig, 1961):

$$\delta^{2}H = 8\,\delta^{18}O + 10 \quad (2)$$

Oxygen and deuterium isotope values show the approximate source of water and illustrate evaporation in groundwater samples. A change in the slope of the relationship between $\delta^{2}H$ and $\delta^{18}O$ can indicate isotopic fractionation of water due to evaporation (Freeze and Cherry, 1979).

To characterize groundwater at the Sand Draw landfill I compared $\delta^{18}O$ and $\delta^{2}H$ ratios from Sand Draw groundwater to the local meteoric water lines of the Wind and Yellowstone Rivers in Wyoming (Coplen and Kendall, 2001), precipitation from Wyoming, Idaho, and Montana (Benjamin et al, 2004), and clayey shallow sediments in the Wind River Range (Jin and Siegel, 2008; Jin, 2008).

Isotopes of Carbon

There are three natural isotopes of carbon; two are stable (^{12}C and ^{13}C) and one is unstable or radioactive (^{14}C). The ratio of $^{13}C/^{12}C$ in groundwater is expressed as $\delta^{13}C$ according to Equation 3 and is measured relative to the $^{13}C/^{12}C$ in a carbonate standard.

$$\boldsymbol{\delta^{13}C = \left[\frac{\left(\frac{^{13}C}{^{12}C}\right)_{sample}}{\left(\frac{^{13}C}{^{12}C}\right)_{standard}} - 1\right] \times 1000} \quad \textbf{(3)}$$

Groundwater $\delta^{13}C$ is affected by fractionation from soil CO_2 diffusion, carbonate dissolution (example in Equation 4), and dilution; when relatively depleted and enriched waters, with respect to $^{13}C/^{12}C$, mix (Mook et al., 1974). These processes naturally skew $\delta^{13}C$ values in groundwater.

$$\mathbf{H^{12}CO_3^- + {}^{13}CO_2\ (g) \leftrightarrow H^{13}CO_3^- + {}^{12}CO_2\ (g)} \quad \textbf{(4)}$$

Fractionation from plant photosynthesis also affects the $\delta^{13}C$of inorganic carbon in groundwater. During photosynthesis ^{13}C is significantly depleted by between 5 and 25 per mil. The amount of fractionation, and ^{13}C depletion, depends on the respiration pathway of a plant. The C_3 pathway accounts for 85 percent of plant species. Temperate and high latitude vegetation is almost exclusively C_3, which also dominates in tropical forests and among major crops including grasses, legumes, and tubers. The C_3 pathway fixes CO_2 using the Rubisco enzyme, which also causes inefficient CO_2 respiration. Most C_3 plant $\delta^{13}C$ values are -27 per mil on average, between -24 and -30 per mil. The more efficient C_4 pathway accounts for less than 5 percent of floral species but is utilized by plants in hot tropical and temperate grasslands including sugar cane, corn, and sorghum. The C_4 pathway uses the PEP carboxylase enzyme to deliver more carbon to Rubisco for fixation, reducing ^{13}C fractionation. C_4 plant $\delta^{13}C$ values are -12.5 per mil on average, between -10 and -16 per mil. The other 10 percent of plants includes desert plants like cacti which can switch between C_3 and C_4 photosynthesis, to photosynthesize during the day and fix CO_2 at night, having intermediate and wide ranging $\delta^{13}C$ values. When this naturally ^{13}C-depleted organic carbon is decays it is incorporated in soils and converted back to CO_2 by aerobic bacteria. The diffusion of microbe-respired CO_2 from the CO_2-rich soil to the

atmosphere causes further fractionation of $\delta^{13}C$ over 4 per mil, enriching the $\delta^{13}C$ of soil CO_2. The $\delta^{13}C$ of environments with C_3 plants is generally -23 per mil, and -9 per mil in C_4 environments (Clark and Fritz, 1997). Buried decayed plant matter is converted to coal which is seen in lenses and seams in Cretaceous and Tertiary geologic formations throughout Wyoming.

Radiocarbon dating is based on the rate of decay of the radioactive carbon isotope ^{14}C which is formed when ^{14}N is bombarded by cosmic neutrons shown in Equation 5. The ^{14}C enters the carbon exchange reservoir (Aitken, 1990) after it is oxidized to $^{14}CO_2$ in the atmosphere or as ^{14}C enters the ocean by atmospheric exchange of carbonate dissolution. Groundwater dating by ^{14}C uses dissolved inorganic and organic carbon entering water as atmospheric $^{14}CO_2$ in the soil zone.

$$\mathbf{^{14}N + neutron \rightarrow {}^{14}C + proton} \qquad \mathbf{(5)}$$

The half-life of ^{14}C is 5730 years and the limit of radiocarbon dating is approximately 50 thousand years. The radioactivity of ^{14}C in dissolved carbon in groundwater is compared to an international standard known as “modern carbon”, which is defined as 95% of the ^{14}C activity in 1950 of the NBS oxalic acid standard. The activity of ^{14}C is expressed as a percent of modern carbon (pMC).

$$\underset{\delta^{13}C = 0‰}{\mathbf{CaCO_3}} \quad + \quad \underset{\delta^{13}C = -25‰}{\mathbf{H_2CO_3}} \quad = \quad \underset{\delta^{13}C = -12.5‰}{\mathbf{2HCO_3^-}} \quad + \quad \mathbf{Ca^{2+}} \qquad \mathbf{(6)}$$

$$\mathbf{pMC = 0\%} \qquad \mathbf{pMC = 100\%} \qquad \mathbf{pMC = 50\%}$$

The pMC of ^{14}C varies as a function of dilution in the same way $\delta^{13}C$ can be diluted. The addition of dead carbon (pMC = 0%) to a solution, from the dissolution of limestone for example, dilutes the pMC of the initial solution. In Equation 6 limestone ($CaCO_3$) with a $\delta^{13}C$ value of 0 per mil and no modern carbon is dissolved by carbonic acid (H_2CO_3) with a $\delta^{13}C$

value of -25 per mil and 100 percent modern carbon. The result is dissolved bicarbonate ($HCO3^-$) with a diluted $\delta^{13}C$ value of -12.5 per mil and a diluted percent modern carbon of 50 percent.

Measured radiocarbon ages are corrected for $\delta^{13}C$ fractionation to a normalized value of -25 per mil relative to the $^{12}C/^{13}C$ ratio in the carbonate standard used in analyses, to account for natural fractionation. Carbon isotopes in groundwater are subject to natural dilution and fractionation from photosynthesis, carbonate dissolution, and mixing. To account for these processes the measured $\delta^{13}C$ is normalized to a value of -25 per mil relative to the $^{12}C/^{13}C$ ratio in the carbonate standard used in analyses. The activity of the measured pMC is then scaled according to the apparent fractionation of $\delta^{13}C$. By measuring the $\delta^{13}C$ and pMC of groundwater, carbon isotopes can constrain the geochemical reactions occurring in a groundwater system and the age of the groundwater can be approximated (Freeze and Cherry, 1979; Clark and Frit, 1997).

Tritium Dating

Radioactive tritium (^3H) consists of an atom of hydrogen in water that has one extra neutron compared to nonradioactive deuterium (^2H). The half-life of Tritium is 12.43 years. Despite this decay, we can still estimate on a decadal scale how long ground water has been in an aquifer since the time it recharged as precipitation. In the 1950's and 60's thermonuclear testing in the south Pacific injected tritiated ocean water into the atmosphere which increased the natural tritium activity (a measure of radioactivity) thousands of times. Tritiated water recharged aquifers all over the world during the period of radioactive testing. This radioactive pulse can now be followed as a tracer in groundwater flow systems. Cosmogenic tritium activity in precipitation prior to the beginning of thermonuclear atomic testing in 1952 is considered 5 - 15 TU. Today, tritium values greater than 5 TU indicate bomb tritium present, tritium values between 1 and 5 TU indicate recently recharged modern water (<5 to 10 years), and tritium

values less than ~1 TU are submodern and recharged prior to 1952. High levels of tritium in groundwater (>10 TU) imply recharge during the 1960s and a presence of bomb tritium. Groundwater with tritium values close to the detection limit (~1 TU) is often paleowater that has mixed with shallow modern groundwater in springs or during monitoring well installation (Freeze and Cherry, 1979; Clark and Fritz, 1997; Motzer, et al., 2006).

Geochemical Modeling

I did inverse mass-balance modeling using NetpathXL, an Excel interface for Netpath, using filtered, radiocarbon dated groundwater samples from shallow monitoring wells at the Sand Draw landfill. Mass-balance groundwater models define the net masses of minerals dissolved or precipitated along a flow path. The chemical evolution of water along a flow path is constrained by the conservation of both mass and electrons. For a detailed explanation and equations for groundwater system reaction models see Plummer et al. (1983).

Netpath uses two inputs, sample chemistry and mineral phases, to constrain multiple mass-balanced geochemical reactions. It models mass-balance reactions between multiple groundwater samples along a real or hypothetical flow path and produces net geochemical reactions that match the geochemistry of the final water sample. Netpath defines the masses (per kg H_2O) of minerals and gases that enter or leave an initial solution constrained by the definition of the final solution:

Initial water + "Reactant Phases" → Final water + "Product Phases"

I used analyses of filtered groundwater samples devoid of organic contamination from the Sand Draw landfill to constrain modeled mineral phases and determined the best Netpath solutions by calibrating models with observed sample $\delta^{13}C$ values. This mass-balance method has been commonly used to correctly define net geochemical reactions in various groundwater

systems by comparing observed and calculated $\delta^{13}C$ values (Plummer and Back, 1980; Back et al., 1983; Plummer and Sprinkle, 2001).

Netpath defines carbon mass balance by Equation 7 and isotopic mass balance by Equation 8 where *R* is the isotopic ratio, *mc* is the total concentration of the element, *I* and *O* are the incoming and outgoing masses of the elements by dissolution/precipitation, and *N* and *M* are the total number of incoming and outgoing phases. For isotopic mass balance the number of incoming phases is indicated by a* and $\alpha_{i\delta}$ is the fraction phase between the i^{th} phases and the solution (Plummer et al., 1994).

$$\boldsymbol{d(m_c) = \sum_{i=1}^{N} dI_i - \sum_{i=1}^{M} dO_i} \quad (7)$$

$$\boldsymbol{d(Rm_c) = \sum_{i=1}^{N} R_i^* dI_i - \sum_{i=1}^{M} R_i \alpha_{i\delta} dO_i} \quad (8)$$

A list of expected mineral phases based on the petrologic studies from Fan et al. (2011) and Neasham and Vondra (1972), and formations and minerals associated with arid environments were used to refine modeled net reactions**.**

Phase	**Stoichiometric Coefficient**									
Halite	Na	1.0	Cl	1.0						
Ion Exchange	Ca	-1.0	Na	2.0	Mg	0.0				
Illite	K	0.6	Mg	0.25	Al	2.3	Si	3.5		
Thenardite	Na	2.0	S	1.0	Redox	6.0				
Calcite	Ca	1.0	C	1.0	Redox	4.0	δC-13	0.0	%C-14	0.0
CO2 Gas	C	1.0	Redox	4.0	δC-13	-25.0	%C-14	100.0		
Dolomite	Ca	1.0	Mg	1.0	C	2.0	Redox	8.0	δC-13	0.0
Na-Mont	Na	0.33	Al	2.33	Si	3.67				
"CH2O"	C	1.0	δC-13	-25.0	%C-14	0.0				
Gypsum	Ca	1.0	S	1.0	Redox	6.0				

Table 2: Stoichiometric coefficients (molar) of constraints in each phase used to refine the Sand Draw net geochemical model. 'Redox' accounts for electron transfer. Isotopic and percent-carbon values are expressed in per mil or percent as appropriate.

The mineral phases included in the NetpathXL model were halite (NaCl), gypsum ($CaSO_4$), calcite ($CaCO_3$), dolomite ($Ca_{0.5}Mg_{0.5}CO_3$), Na-montmorillonite, thenardite (Na_2SO_4), atmospheric CO2gas and organic carbon ("CH_2O") (stoichiometric coefficients shown in Table 2). Because potassium feldspar and plagioclase phases have dissolution rates multiple orders of magnitude slower than carbonates they were not included in Netpath modeling (Pokrovsky and Schott, 2001; Stillings et al., 1996; Berner and Morse, 1974).

Sand Draw Landfill Dataset												
WELL	**Ca**	**HCO3**	**Cl**	**Mg**	**K**	**Na**	**SO4**	**SC**	**δC-13**	**δO-18**	**δH-2**	**Tritium**
R-7	98.5	158.0	17.0	6.1	2.7	695.0	4500.0	3500		-18.74	-148.5	2.3
R-8	379.0	80.0	164.0	24.6	0.3	553.0	2030.0	4120		-16.38	-136.9	1.64
R-9D	170.0	530.0	37.0	10.0	2.7	393.0	832.0	2320	-10.8	-15.90	-132.8	<0.8
R-10	8.0	260.0	4.0	0.6	1.1	173.0	127.0	814		-18.61	-148.3	<0.8
R-11	6.2	184.0	4.0	0.5	1.0	106.0	100.0	533		-16.02	-130.4	7.9
R-12	114.0	37.0	84.0	2.6	3.7	761.0	1790.0	3850	-21.0	-15.61	-127.3	<0.8
R-18	126.0	172.0	13.0	9.8	2.6	214.0	653.0	1560	-7.7	-16.75	-137.6	<0.8
R-20	358.0	151.0	17.0	37.1	5.9	1620.0	4700.0	7810	-19.3	-17.10	-140.3	0.93

Table 3: A laboratory analysis of nine wells provided the chemical dataset constraining the NetpathXL model. Carbon isotope values were measured at four wells. All analyses are in mg/L and isotopic analyses are measured in permil. Because Netpath modeling was constrained by the measured carbon-13 in each sample only wells with measured carbon-13 values were used in modeling.

Basic Precipitation and Dissolution Reactions Involving Organic Carbon	
(Ca,Mg)/Na Ion Exchange	$\mathbf{(Ca, Mg)^{2+} + Na_2\text{-}Clay = 2Na^{2+} + (Ca, Mg)\text{-}Clay}$
Calcite Dissolution	$\mathbf{CaCO_3 + H_2CO_3 = Ca^{2+} + 2HCO_3^-}$
Dolomite Dissolution	$\mathbf{CaMg(CO_3)_2 + 2H_2CO_3 = Ca^{2+} + Mg^{2+} + 4HCO_3^-}$
Epsomite Dissolution	$\mathbf{MgSO_4 + 2CH_2O = Mg^{2+} + H_2S^- + 2HCO_3^-}$
Thenardite Dissolution	$\mathbf{Na_2SO_4 + 2CH_2O = 2Na^+ + H_2S^- + 2HCO_3^-}$
Bicarbonate Precipitation	$\mathbf{2CH_2O + SO_4^{2-} = H_2S^- + 2HCO_3^-}$

Table 4: Netpath modeling precipitates or dissolves the basic mineral phases constraining the model based on the chemical constraints given from samples. Shown here are the basic precipitation and dissolution reactions, and ion exchange, that affect organic carbon.

Initial precipitation was modeled as slightly acidic (pH 5.7) with 0.01 mg/L alkalinity and $\delta^{13}C$ TDIC of 25‰ and pMC TDIC of 100 percent. Final groundwater samples were defined by

Sand Draw sample chemistry (Table 3). Basic precipitation and dissolution reactions involving organic carbon and carbon acid (H_2CO_3) are shown in Table 4.

Netpath calculates the adjusted $\delta^{14}C$ activity of groundwater by initially assigning additive fractionation factors twice that of the $\delta^{13}C$.factor for processes involving carbon. Netpath modeling attempts radiocarbon dating of a final groundwater sample using the age of the initial $\delta^{14}C$ of the precipitation recharge, A_0, the adjusted $\delta^{13}C$ of the final well, and the measured $\delta^{14}C$ content of the final water, A, using Equation 9. Netpath computes A_{nd} for each reaction model using A_0, the defined $\delta^{14}C$ and fractionation factors of carbon sources, and computed carbon-mass transfer. The calculated $\delta^{14}C$ is the travel time between the initial precipitation recharge and final water samples and is comparable to the measured apparent age of the water sample. Initial $\delta^{14}C$ is calculated by mass-balancing carbon sources (calcite, and dolomite) and CO_2 gas, assuming carbon sources have 0 percent modern carbon and CO_2 gas has 100 percent modern carbon. NetpathXL reports carbon-14 values in percent modern carbon (pMC) (Plummer et al., 1994).

$$\Delta t(\mathbf{years}) = \frac{5730}{\ln 2} \ln\left(\frac{A_{nd}}{A}\right) \quad \textbf{(9)}$$

The chemical analysis of each Sand Draw well is shown in Table 3. The Sand Draw water samples were charged balanced for speciation in NetpathXL. Only four of these wells (R-9D, R-12, R-18, and R-20) were used in NetpathXL modeling because of the availability of $\delta^{13}C$ and pMC data. The locations of wells at the Sand Draw landfill are shown in Figure 6. Samples from wells R-9D, R-12, R-18 and R-20 were taken at depths of 60, 50, 52, and 55 feet deep respectively.

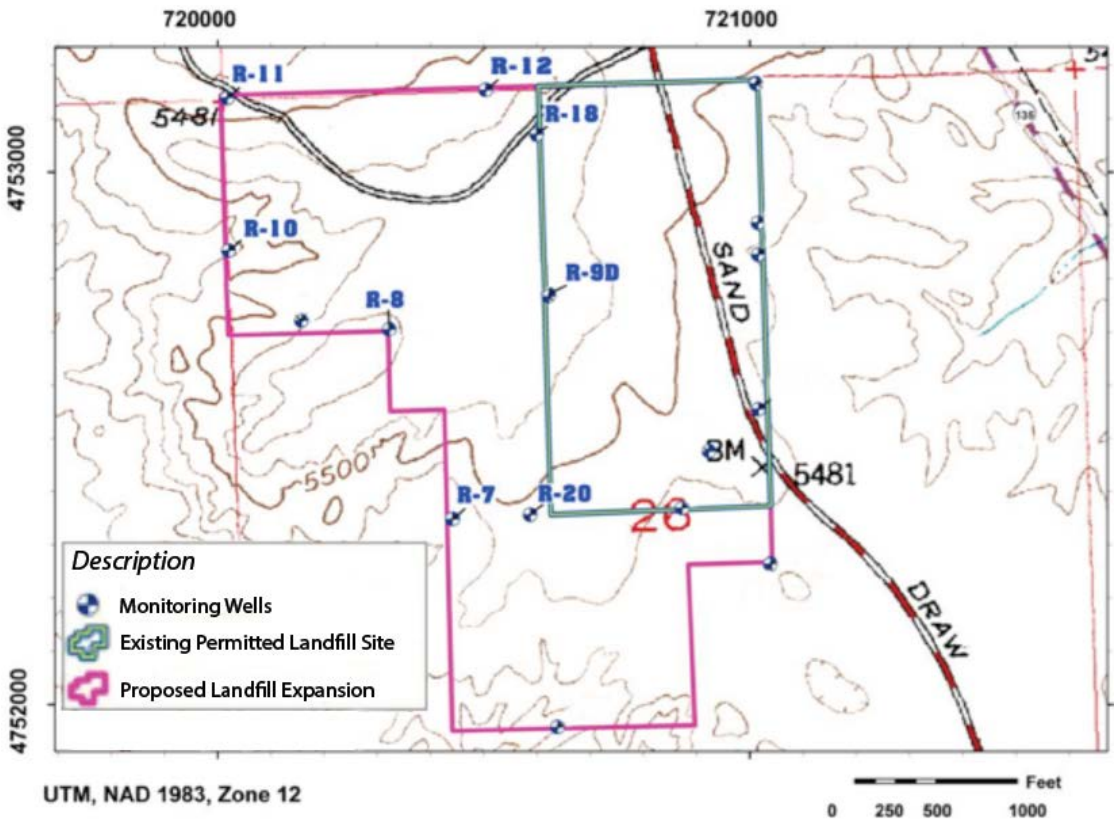

Figure 6: A map of the Sand Draw landfill showing the locations of wells used in NetpathXL modeling (Modified after Siegel, 2011).

Model Input Significance Testing

To test the robustness of Netpath geochemical modeling a significance test of model inputs involving carbon was done (Appendix A). Initial sample conditions and phases were changed to see the relative effect slight model adjustments have on the adjusted age of samples.

Modeling adjustments in the initial water sample included a pH of 5.7 ± 1 unit, an increase and decrease in alkalinity/TDIC of 0.001 mg/L by one order of magnitude, an increase in $\delta^{13}C$ from -25 per mil to -17 and -12 per mil, and a decrease in pMC from 100 percent to 50 percent. Calcite and dolomite phase $\delta^{13}C$ was 0 ± 1 per mil and the $\delta^{13}C$ values of atmospheric CO_2 and organic carbon was increased from -25 per mil to -17 and -12 per mil. The pMC of organic carbon was increased from 0 percent to 50 and 100 percent.

Results and Discussion

Statewide Geochemical Patterns in Landfills

An initial analysis of groundwater quality from landfills included in the WDEQ report in different basins (see map Figure 1) shows MCL or GPS exceedances of ammonia, chloride, iron, manganese, sodium, and sulfate in unfiltered WDEQ samples (Table 5). Examples of chloride, sodium, and sulfate exceedances in the WDEQ dataset can be seen in Figure 7. Additional bivariate analyses are in Appendix B.

Parameter	GPS or MCL (mg/L)	Percent Exceedances
Ammonia[1]	0.5	53.62
Chloride	250.0	20.35
Iron	0.3	91.58
Manganese	0.05	90.53
Sodium[2]	60.0	77.77
Sulfate	250.0	63.71

Table 5: A percentage of WDEQ samples exceeded the GPS or MCL for certain parameters. Not all WDEQ samples had complete chemical analyses and the percent exceedances among samples only reflects the percent of samples with paramter concentrations at or above the GPS or MCL relative to the total number of samples with certain perameter measurements. 1. The GPS for ammonia according to WDEQ Water Quality Rules and Regulations (WDEQ, 2007) 2. The GPS for sodium acccording to EPA Driking Water Standards and Health Advisories (EPA, 2012).

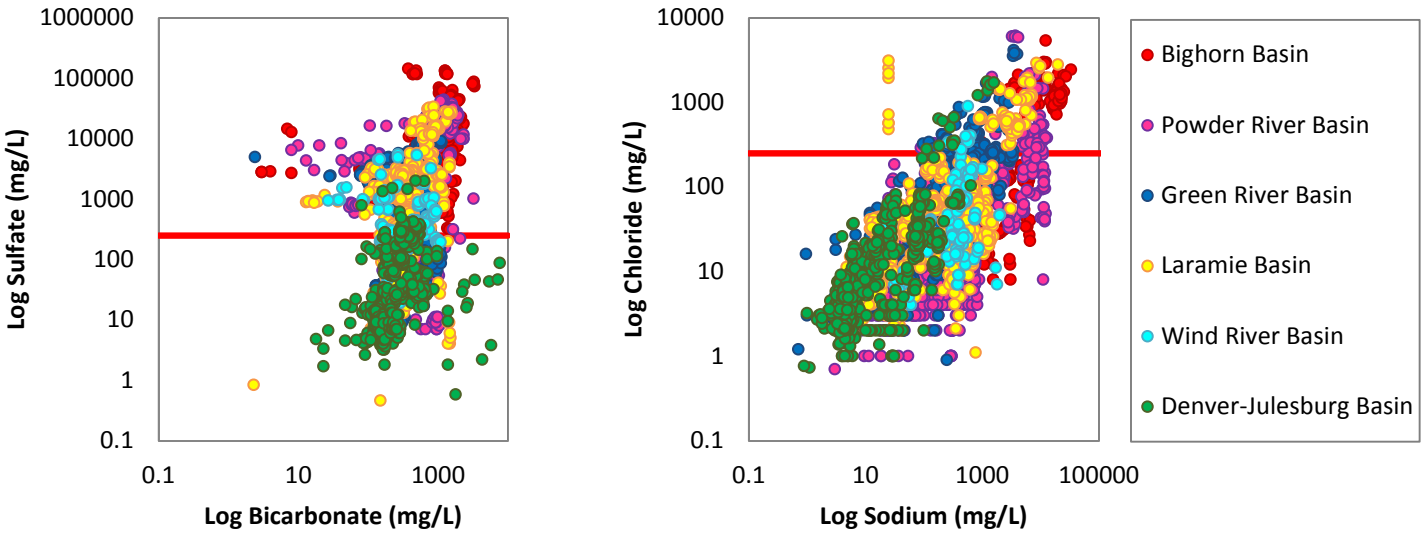

Figure 7: Graphs of log-Bicarbonate vs. log-Sulfate and log-Sodium vs. log-Chloride data for landfills in each basin. Red lines are at the EPA maximum contaminant levels for sulfate and chloride, both of which are 250 mg/L. (Sulfate MCL, Chloride MCL: WDEQ, 2007; Data: WDEQ, 2010).

Piper diagrams show the hydrochemical facies of groundwater differs between basins, ranging from calcium-bicarbonate to sodium-sulfate (Figure 8). There are no apparent geochemical differences between contaminated and uncontaminated sites (Figure 9).

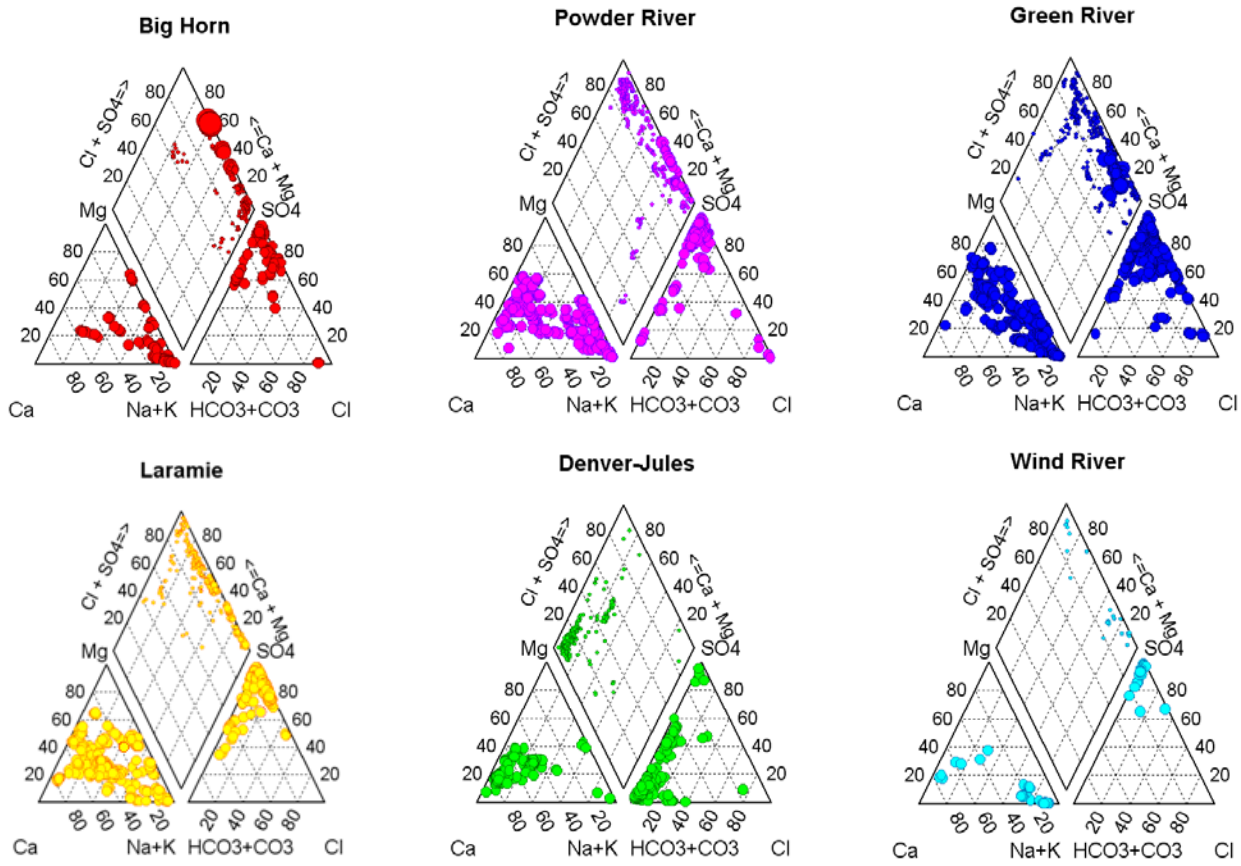

Figure 8: Piper diagrams show that the hydrochemical facies of groundwater changes among basins across Wyoming. The facies of groundwater range from calcium bicarbonate water in the Denver-Jules basin to sodium sulfate groundwater in the Big Horn, Green River, and Wind River basins. In the central diamond of each piper diagram sample point size differences indicate varying amounts of total dissolved solids in each sample (Data: WDEQ, 2010).

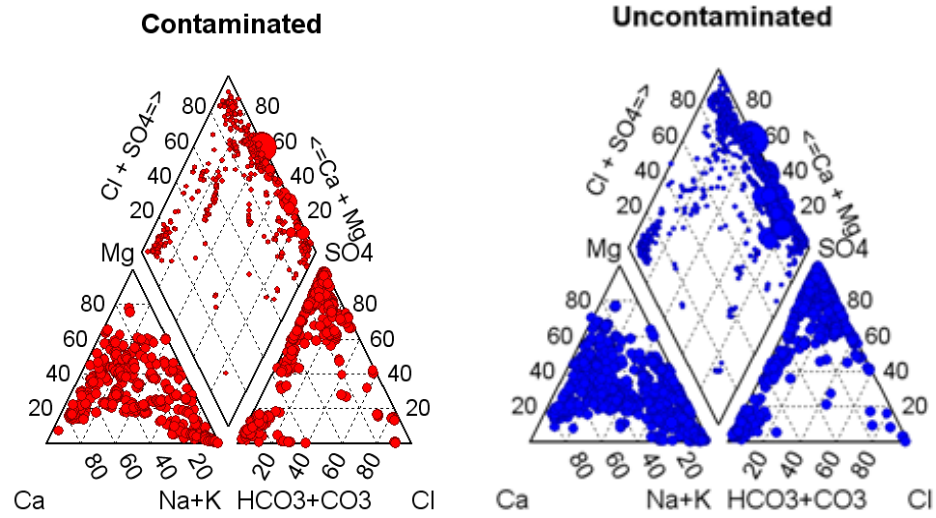

Figure 9: The hydrochemical facies in groundwater samples contaminated with VOCs is not different compared to the hydrochemical facies of uncontaminated groundwater (Data: WDEQ, 2010).

In groundwater contaminated by landfill leachate, chemical trends should be consistent with typical landfill reduction-oxidation reactions (Table 1) and increases in common leachate indicators such as TOC and ammonia (Christensen, et al., 2001). Both contaminated and uncontaminated groundwater samples do not show the expected increases in landfill leachate indicators when compared to chloride, a conservative chemical indicator of leachate contamination expected in leachate as a byproduct of organic waste decomposition. The correlation between TOC and chloride (R^2 = 0.22 and 0.20) and the correlation between Ammonia and chloride (R^2 = 0.14 and 0.04) are both low (Figure 10).

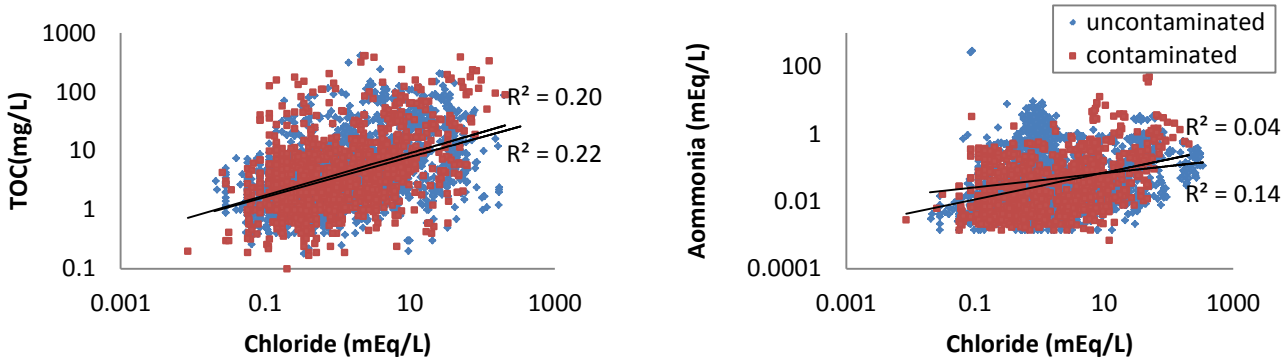

Figure 10: A comparison of samples from sites the WDEQ identified as contaminated (VOCs present) or uncontaminated show no logical trends expected of typical landfills geochemical processes distinguishing contaminated and uncontaminated sites. A positive correlation between TOC and ammonia, and chloride, would commonly indicate landfill processes are occurring however no apparent difference between uncontaminated and contaminated groundwater samples is seen.

Furthermore, groundwater contaminated with VOCs from landfilled solvents, paint, and cleaning supplies etc. do not show the expected increases in chloride (R^2 = 0.03) and TOC (R^2 = 0.02) as total VOC concentrations increase (Figure 11). There are no logical trends when common leachate indicators are compared to the total amount of VOCs in contaminated water samples. Because of the lack of expected geochemical relationships between chloride, other leachate indicators, and the presence of VOCs, only VOCs can be used to reliably indicate leachte-groundwater interaction.

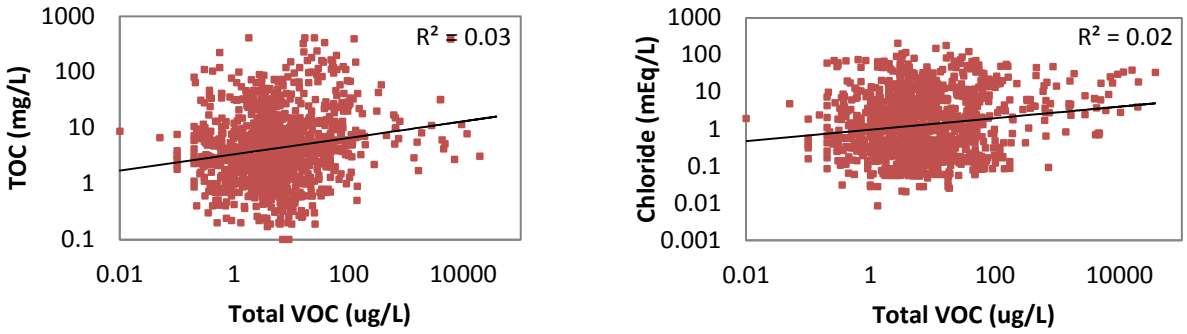

Figure 11: A comparison of TOC and chloride to the amount of total VOCs in samples from the WDEQ dataset show no logical trends expected from common leachate contamination

Although inconsistent with common leachate indicators, geochemical trends also differed among landfills that receive different types of waste (Figure 12). Between landfill types the correlation between ammonia and chloride (R^2 = 0.11 and 0.14) and between TOC and chloride (R^2 = 0.06, 0.20, and 0.56) are also low. The highest correlation (R^2 = 0.56) was between TOC and chloride among landfills receiving construction waste, a relatively small dataset with low TOC levels compared to sanitary and industrial-waste landfills.

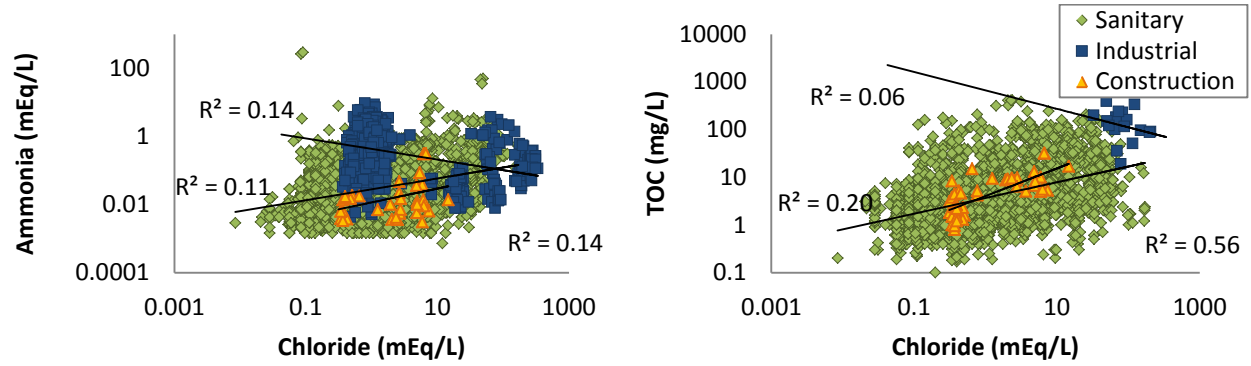

Figure 12: Geochemical trends differ between landfills receiving different types of waste. The relationships between ammonia, TOC, and chloride do not differ among contaminated or uncontaminated landfills however difference between different landfill types can be seen.

Bivariate plots of chemical relationships representing different solute relationships vary among landfill types (Figure 13). These correlations were used to constrain geochemical modeling processes along with reviewed literature.

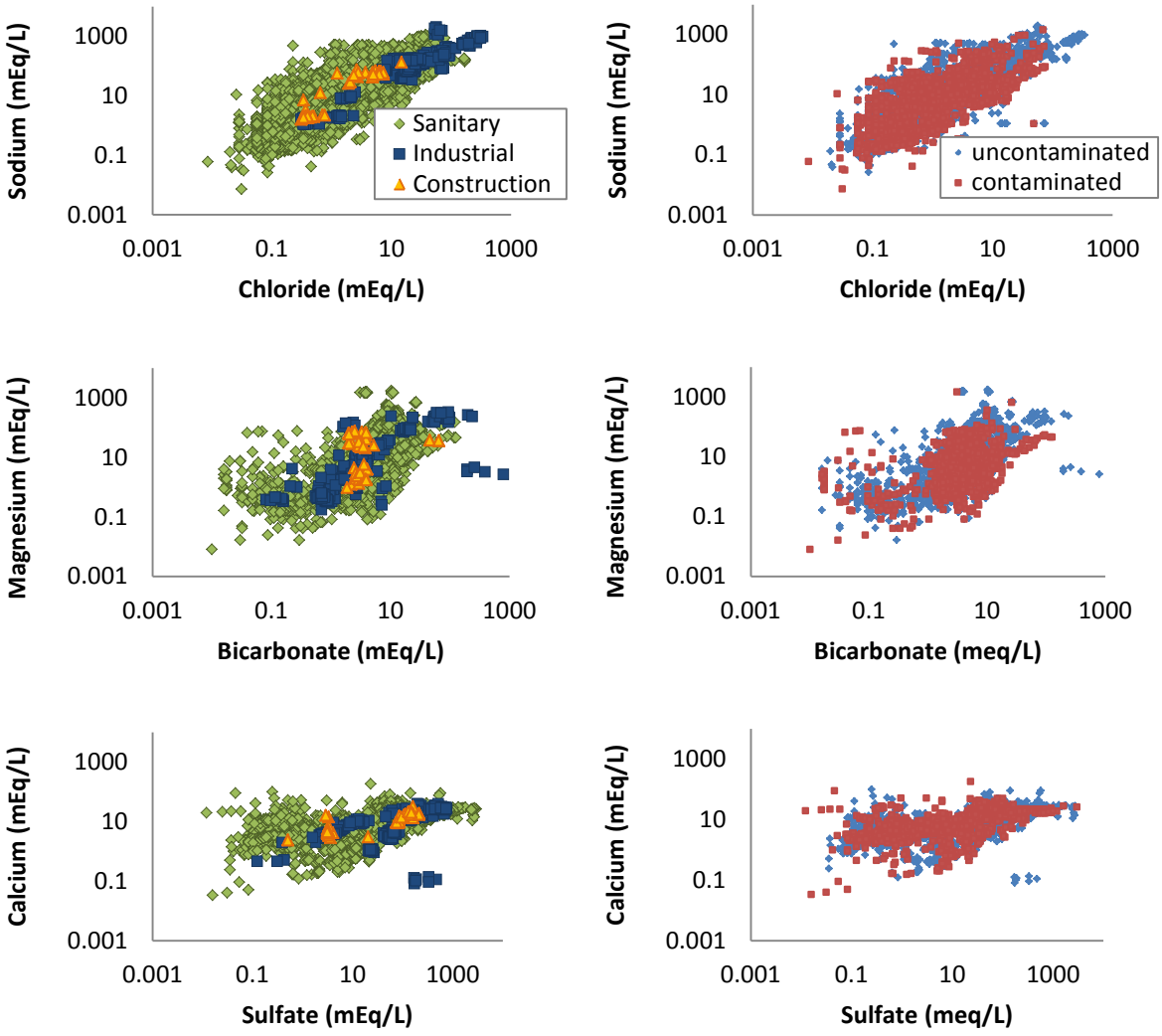

Figure 13: These bivariate plots show comparisons of the concentrations of solutes among different landfill types and landfill contamination conditions from the WDEQ dataset. There does not appear to be a relationship between contamination status and solute concentration. The variability of solute relationships changes between landfill types.

Thermodynamically plausible iron and manganese concentrations are derived from the fields of stability of equilibrium dissolved iron and manganese activity as a function of pH. For a range of pH values the thermodynamically plausible equilibrium activity of both iron and manganese changes by orders of magnitude (Hem, 1985). A large set of WDEQ sample total iron and total manganese values exceed the maximum possible concentrations by orders of magnitude (Figure 14). These extreme metal values do not realistically reflect natural iron and manganese concentrations in groundwater samples and may be due to increased colloid mobility in oxizing

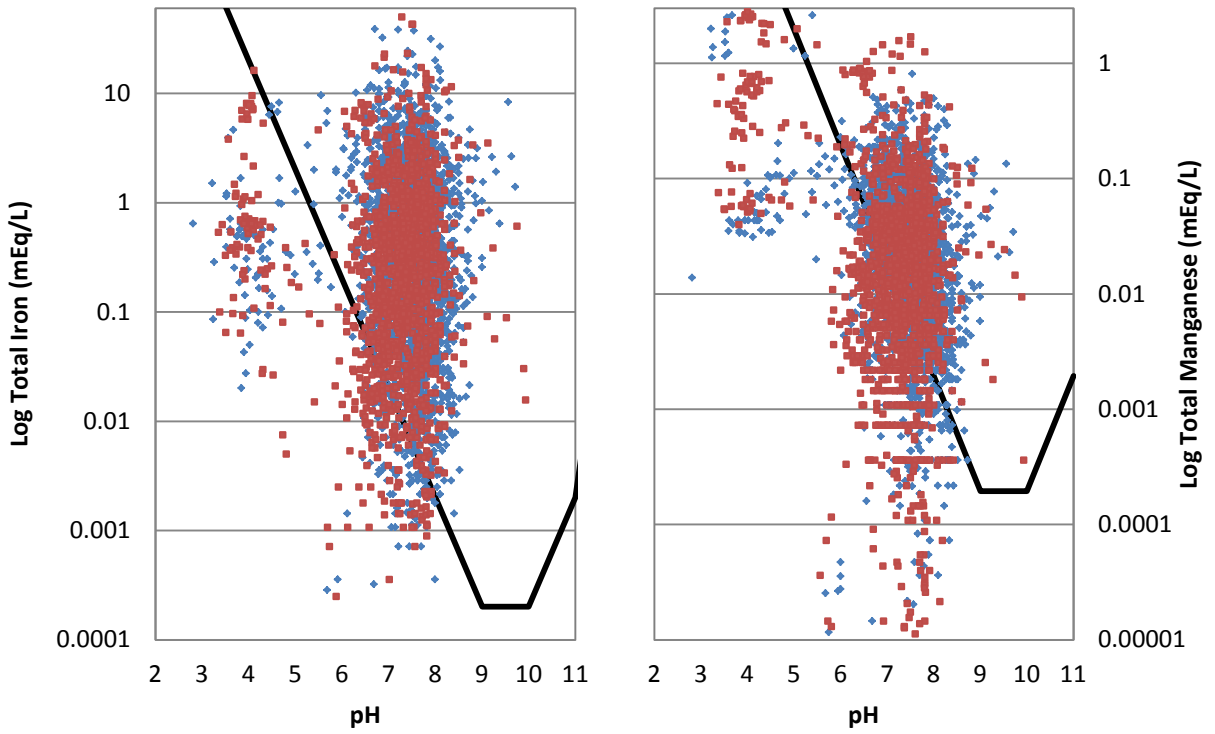

Figure 14: Comparisons of total iron and total manganese values and pH for uncontaminated (blue) and contaminated (red) WDEQ water samples. The maximum concentration of iron and manganese thermodynamically possible is indicated by a line (black) derived from Hem (1985). Note the large set of data plotting orders of magnitude higher than the highest thermodynamically stable value.

conditions or increased turbidity as a result of pumping or well construction. Under reducing conditions the presence of colloids may represent natural metal transport (Saar, 1997). Filtration reduces total metal concentrations as filter sizes decrease, and filtered samples are representative of less turbid groundwaters (Gibb, et al., 1981).

A broad geochemical analysis of groundwater samples from landfills contaminated or uncontaminated, with respect to the presence ot VOCs, show that common inorganics found in landfill leacte are less reliable at distinguishing landfil leachate contamination in groundwater compared to the presence of VOCs. Furthermore, sampling protocols requiring unfiltered groundwater samples for metal analyses result in erroneous iron and manganese vaules.

Geochemical Modeling

The results of Netpath mass-balance modeling are showin in Appendix C. Netpath modeling produced 10 functional models using the expected mineral phases and chemical constraints for each well. For each well multiple modeled $\delta^{13}C$ isotope values calibrated models to observed $\delta^{13}C$ isotope values. Isotopic calibration indicates that the modeled geochemical mass-balance reactions plausibly could result in the final chemistry seen in each well.

The results of Netpath modeling are the stoichiometric coefficients in mmol/L H_2O that dissolve (positive coefficients) or precipitate (negative coefficients) to/from solution as it evolves along a flow path. Because of the chemical constraints given in Netpath modeling some mineral phases do not change behavior between model results for a single well. Other mineral phases change relative to one another because multiple mineral phases may contain different combinations of the same elements constrained by well chemistry.

Sand Draw landfill samples did not contain silicon or aluminum analyses to constrain argillaceous illite and montmorillonite phases so the modeled mass balance of these phases represents ion exchange from calcium, magnesium, and sodium ions in clay. For example, it should be understood that the appearance of Na-montmorillonite precipitation (a negative coefficient shown in Appendix A) is the removal of sodium ions from groundwater.

From the Netpath modeling results it is seen that, for multiple $\delta^{13}C$-calibrated models at each well, it is plausible that natural geochemical reactions produced the chemical concentrations seen in Sand Draw groundwater samples. The observed and calculated (adjusted) radiocarbon values are shown in Table 6. In each well all models were calibrated and have equal measured and calculated carbon-13 values. The computed carbon-14 pMC values from Netpath modeling are between 13 and 36 percent higher than observed pMC. Groundwater ages adjusted by

Netpath modeling are between 28 and 56 percent younger than previously measured, uncorrected ages.

Well	Observed			Computed		
	Carbon-13	C-14 pMC	Measured Age (years)	Carbon-13	C-14 pMC	Adjusted Age (years)
R-9D	-10.8	6	21900	-10.8	43	15599^{+6067}_{-13119}
R-12	-21	57	4480	-21	84	3169^{+60}_{-1594}
R-18	-7.7	12	16900	-7.7	31	7656^{+6067}_{-6472}
R-20	-19.3	63	3650	-19.3	77	1618^{+94}_{-1281}

Table 6: Netpath results for carbon dating adjustment show that groundwater ages corrected by modeling are hundreds to thousands of years older than modern recharge.

These old ages for groundwater agree with the interpretation of stable isotopes of water. The isotopes of groundwater from the Sand Draw landfill plots in an evaporative trend below the local meteoric water line from the Wind River (Figure 15). The Wind River and Yellowstone River $\delta^{18}O$ values intersect the local meteoric water line at approximately -20 per mil, near the average $\delta^{18}O$ values for snowmelt and shallow groundwater in Wind River Basin (Jin and Siegel, 2008; Jin, 2008). Sand Draw groundwater intersects the local meteoric waterline at a $\delta^{18}O$ value

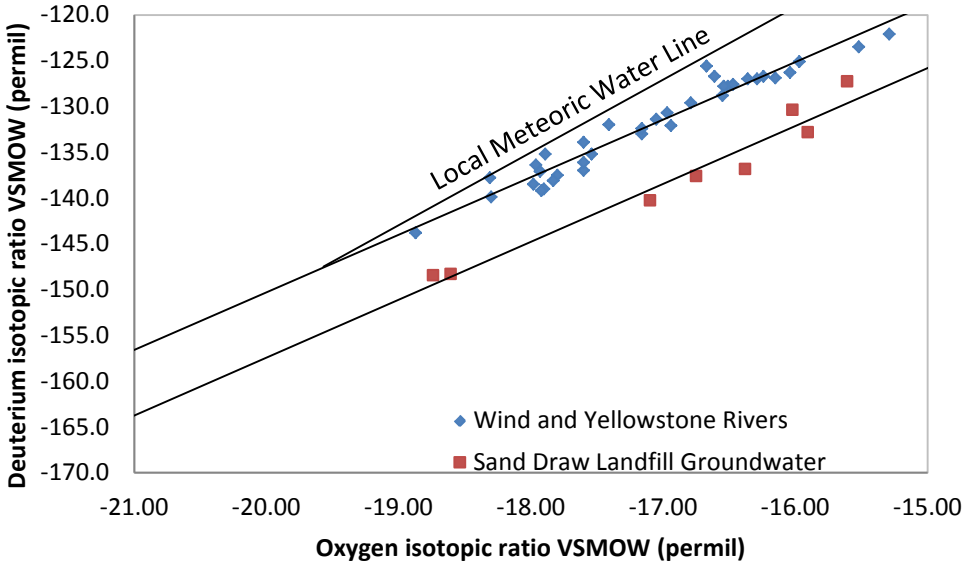

Figure 15: The Sand Draw groundwater deuterium and oxygen isotopic values plot below Wind and Yellowstone River isotopic values on an evaporative trend relative to the local meteoric water line of precipitation from Wyoming, Idaho, and Montana (Jin and Siegel, 2008; Jin, 2008).

of approximately -24 per mil prior to evaporation, which is smaller than for modern snowmelt recharge and more comperable to glacial ice or rain that recharged Wind River groundwater under colder conditions thousands of years ago (Person et al., 2007). Futhermore, the tritium values of radiocarbon dated groundwater samples fall below or within the range of tritium activity prior to thermonuclear testing (less than ~1 TU) indicating that most of the water that recharged the sandy sediments penetrated by the monitoring wells occurred at least 50 years ago, suggesting minimal modern recharge (Table 3). The tritium values of other groundwater samples that were not radiocarbon dated vary between paleowater (<0.8 TU), modern recharge (1.64 TU and 2.3 TU), and bomb-tritiated recharge (7.9 TU). It is plausible that tritiated waters used in monitoring well installation at the landfill mixed with existing submodern groundwaters (Clark and Fritz, 1997).

The results of significance testing carbon-constrained model inputs (Appendix A) show that modeled ages are only significantly affected by adjustments in the $\delta^{13}C$ value of CO_2 gas and organic carbon (Figure 16). The geochemical model did not always compute sensible ages for some samples using atmospheric CO_2 and organic carbon $\delta^{13}C$ values of -12 and -17 per mil. In spite of the sensitivity of age adjustement to changes in input $\delta^{13}C$ the adjusted ages of samples are consistently younger

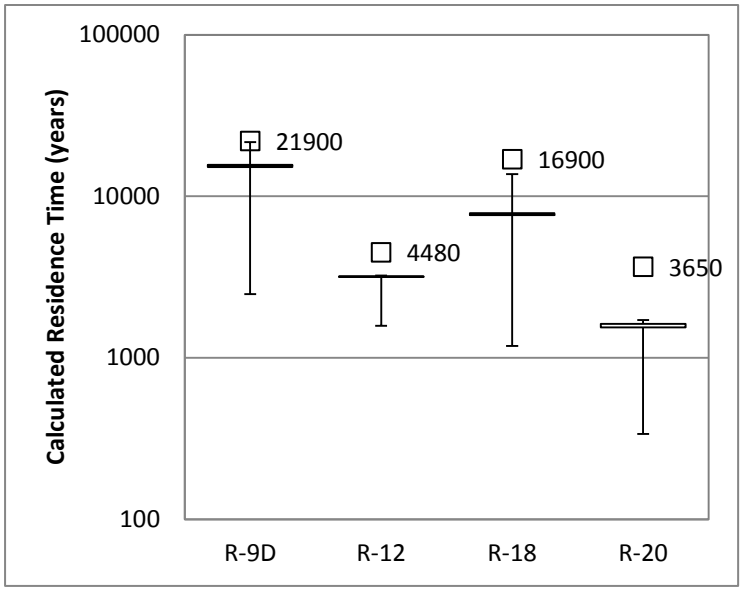

Figure 16: The results of significance testing model inputs show the error associated with model inputs. Most of the model inputs constrained by carbon do not significantly affect age adjustment results. An increase in the $\delta^{13}C$ of atmospheric CO_2 and organic carbon from -25 per mil to -17 and -12 per mil introduce a wide range of error to modeling results. However, the adjusted ages of groundwater samples are still hundreds to thousands of years older than modern recharge and all groundwater ages adjusted by modeling are consistently younger than initially observed (squares).

than previously observed and remain hundreds to thousands of years older than modern recharge for a range of input $\delta^{13}C$ vaules.

Conclusions

High concentrations of solutes in groundwater samples from monitoring wells between contaminated and uncontaminated landfills show that high solute concentrations do not necessarily indicate groundwater contamination. In an arid environment salt dissolution and evapoconcentration create the conditions for naturally high concentrations of solutes. Without the co-occurrence of VOCs, exceedences of MCLs of major solutes cannot be used as a means to identify contamination from Wyoming landfill leachate. Furthermore, sampling protocols and treatment used by the WDEQ, specifically not filtering samples to remove particulate material prior to analysis, produces erroneous trace metal results that cannot be used to determine leachate-groundwater contamination.

Mass-balance modeling constrained by well chemistry and calibrated using $\delta^{13}C$ at the Sand Draw landfill, a "typical" municipal solid waste landfill, shows that natural geochemical reactions could have plausibly produced the concentrated sodium-sulfate water seen at the Sand Draw landfill and typical of valley fill deposits between major mountain ranges and underlying landfills in Wyoming.

Oxygen and deuterium isotopic results and radiocarbon dating results combined show that groundwater under the Sand Draw landfill is thousands of years older than modern recharge. The disconnect between Sand Draw groundwater samples and local shallow groundwater suggests that Sand Draw groundwater samples are from a separate paleowater aquifer possibly perched above regional groundwater. The disconnectedness of a perched groundwater zone at the Sand Draw landfill is analogous to the groundwater below other Wyoming landfills constructed

on basin fill. It is reasonable to assume that leachate contamination from landfills throughout Wyoming cannot reasonably reach most independent perched water zones, let alone the deeper regional water table, in human lifetimes.

Combined, the geochemical evaluation of the WDEQ landfill monitoring well dataset coupled to my case study of the Sand Draw landfill shows that contamination of groundwater by landfill leachate in Wyoming only can be considered plausible if VOCs can be identified unless sampling protocols are changed to properly capture geochemical changes derived from landfill processes.

Future Work and Recommendations

It is recommended that the WDEQ filter all groundwater samples prior to analyses based on the erroneous metal values seen in unfiltered samples. When an unfiltered, turbid sample is acidified according to WDEQ protocol unfiltered sediment from limestone, gypsum, dolomite, and silt and claystone particles unnaturally dissolve into solution. The acidification of an unfiltered, especially turbid sample may increase solute concentrations above naturally representative levels.

Recommended future work includes further sampling and mass-balance modeling. Future work may include a comparison of filtered and unfiltered samples from identical landfill monitoring wells and between landfills in different geologic settings. Comparing the accuracy of different sample protocols in different geologic settings may show that sampling protocols should be tailored to the setting that water samples are being analyzed from. It may be important to pursue developing separate sample analysis techniques for landfills in different climate and geologic environments.

Future mass-balance modeling using Netpath may be constrained with S^{34} isotopic values if available. Other constrains that were not available but would have improved model results include aluminum and silica. Calibrating model constraints to the stratigraphy and mineralogy of the sampling location, from well boring logs, would also increase model relevance for specific water samples.

Appendices

Initial Sample				Inputs								Conditions	R-9D	R-12	R-18	R-20
				Calcite		CO2 Gas		Dolomite		"CH2O"						
pH	Alk/TDIC	C-13 TDIC	C-14 TDIC	I1	I2	I1	I2	I1	I2	I1	I2					
5.7	0.001	25	100	0	0	-25	100	0	0	-25	0	Initial	15599	3173	7658	1618
6.7	0.001	25	100	0	0	-25	100	0	0	-25	0		15599	3170	7657	1618
4.7	0.001	25	100	0	0	-25	100	0	0	-25	0		15602	3198	7674	1625
5.7	0.01	25	100	0	0	-25	100	0	0	-25	0		15603	3204	7677	1627
5.7	0.0001	25	100	0	0	-25	100	0	0	-25	0		15599	3169	7657	1618
5.7	0.001	17	100	0	0	-25	100	0	0	-25	0		15599	3172	7658	1618
5.7	0.001	12	100	0	0	-25	100	0	0	-25	0		15599	3172	7658	1618
5.7	0.001	25	50	0	0	-25	100	0	0	-25	0		15599	3173	7658	1618
5.7	0.001	25	100	1	0	-25	100	0	0	-25	0	Calcite Only	16007	3233	8343	1712
5.7	0.001	25	100	-1	0	-25	100	0	0	-25	0	Calcite Only	15133	3107	6846	1516
5.7	0.001	25	100	0	0	-17	100	0	0	-25	0	With CH2O	6494	Error	Error	952
5.7	0.001	25	100	0	0	-17	100	0	0	-25	0	Without CH2O	18787	Error	10846	error
5.7	0.001	25	100	0	0	-12	100	0	0	-25	0	With CH2O	2480	Error	8678	Error
5.7	0.001	25	100	0	0	-12	100	0	0	-25	0	Without CH2O	21666	Error	13725	Error
5.7	0.001	25	100	0	0	-25	100	1	0	-25	0	Dolomite Only	16007	3233	8343	1712
5.7	0.001	25	100	0	0	-25	100	-1	0	-25	0	Dolomite Only	15133	3107	6846	1516
5.7	0.001	25	100	0	0	-25	100	0	0	-17	0	With CH2O	13481	n/a	n/a	337
5.7	0.001	25	100	0	0	-25	100	0	0	-17	0	Without CH2O	15599	3173	7658	1618
5.7	0.001	25	100	0	0	-25	100	0	0	-12	0	With CH2O	14745	1579	1186	1086
5.7	0.001	25	100	0	0	-25	100	0	0	-12	0	Without CH2O	15599	3173	7658	1618
5.7	0.001	25	100	0	0	-25	100	0	0	-25	50		9869	n/a	1929	n/a
5.7	0.001	25	100	0	0	-25	100	0	0	-25	100		15599	3173	7658	1618

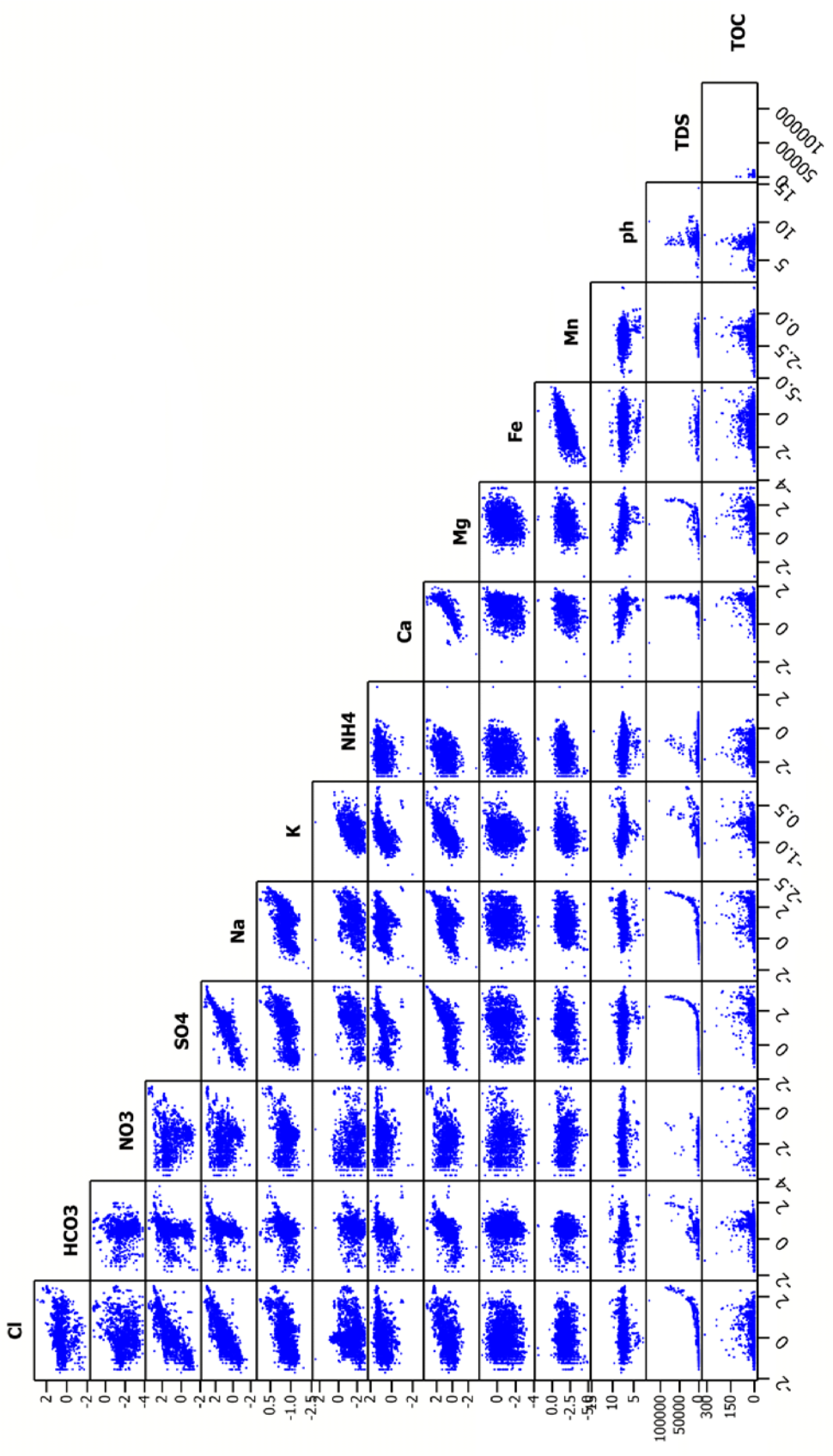
Uncontaminated Well Data
Cl
HCO3
NO3
SO4
Na
K
NH4
Ca
Mg
Fe
Mn
ph
TDS
TOC
Data is presented in log mEq; pH in s.u.; TDS, TOC in log mg/L; VOC in log ug/L

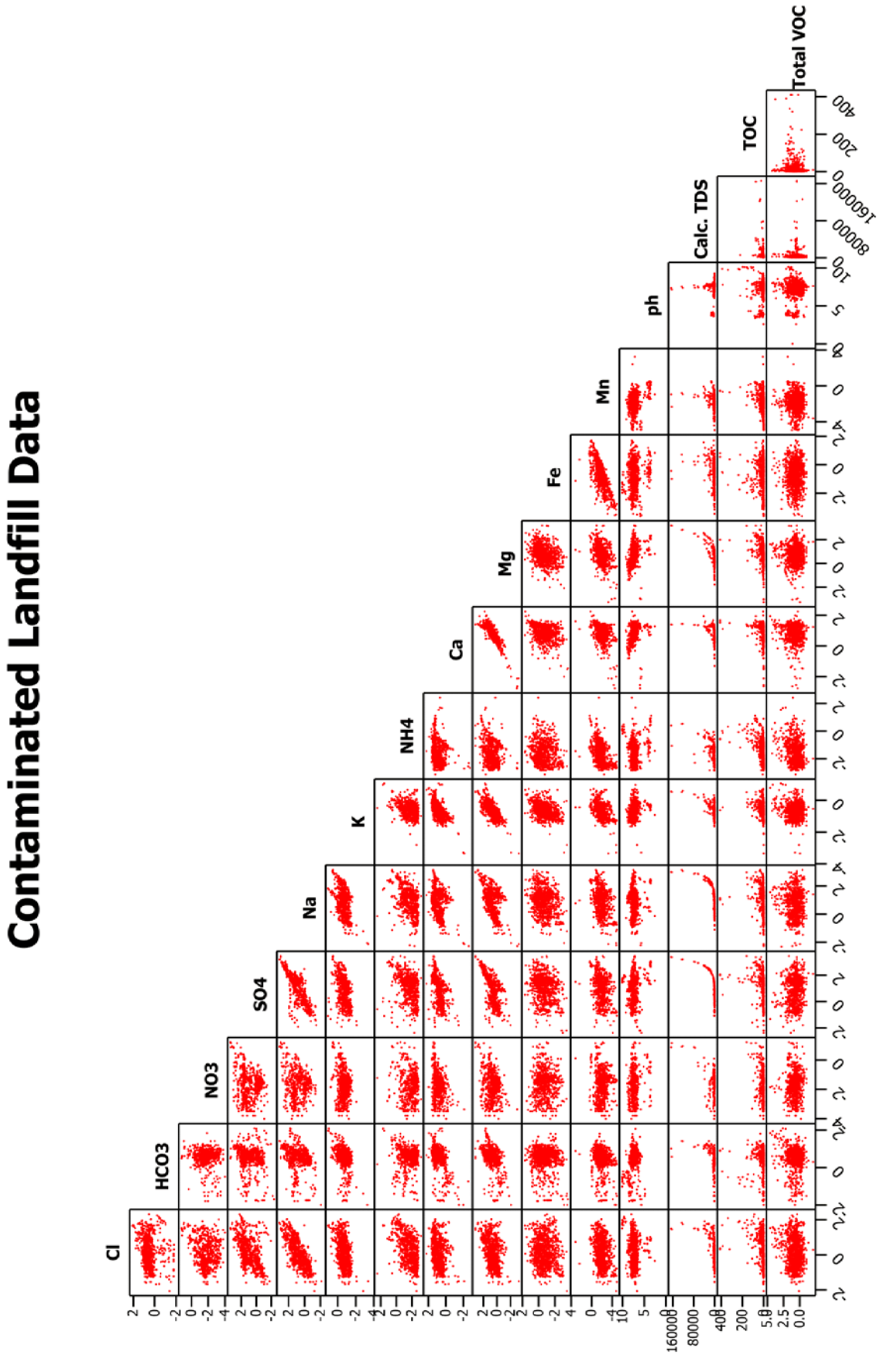
Contaminated Landfill Data
Cl
HCO3
NO3
SO4
Na
K
NH4
Ca
Mg
Fe
Mn
ph
Calc. TDS
TOC
Total VOC
Data is presented in log mEq; pH in s.u.; TDS, TOC in log mg/L; VOC in log ug/L

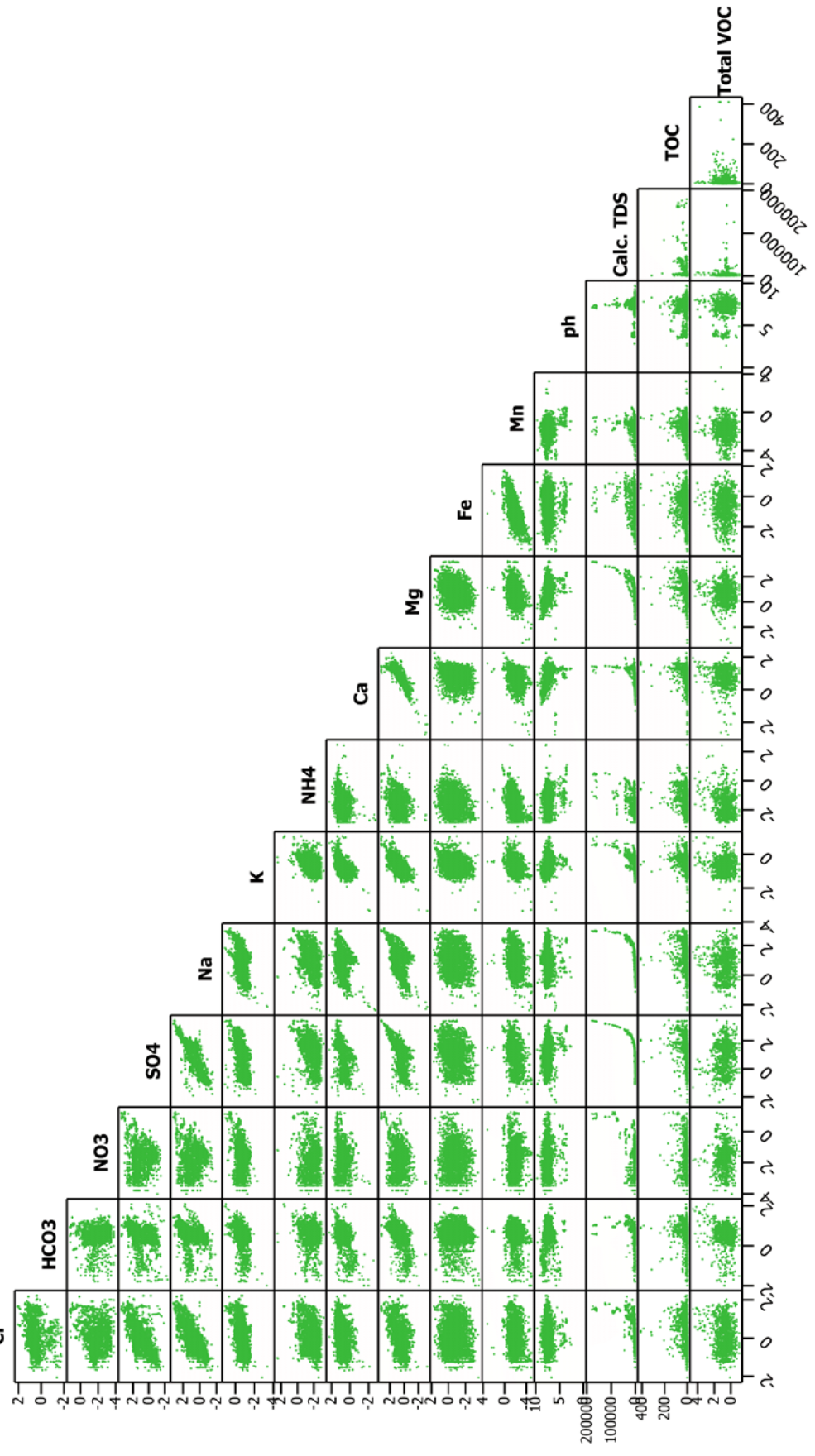

Data is presented in log mEq; pH in s.u.; TDS, TOC in log mg/L; VOC in log ug/L

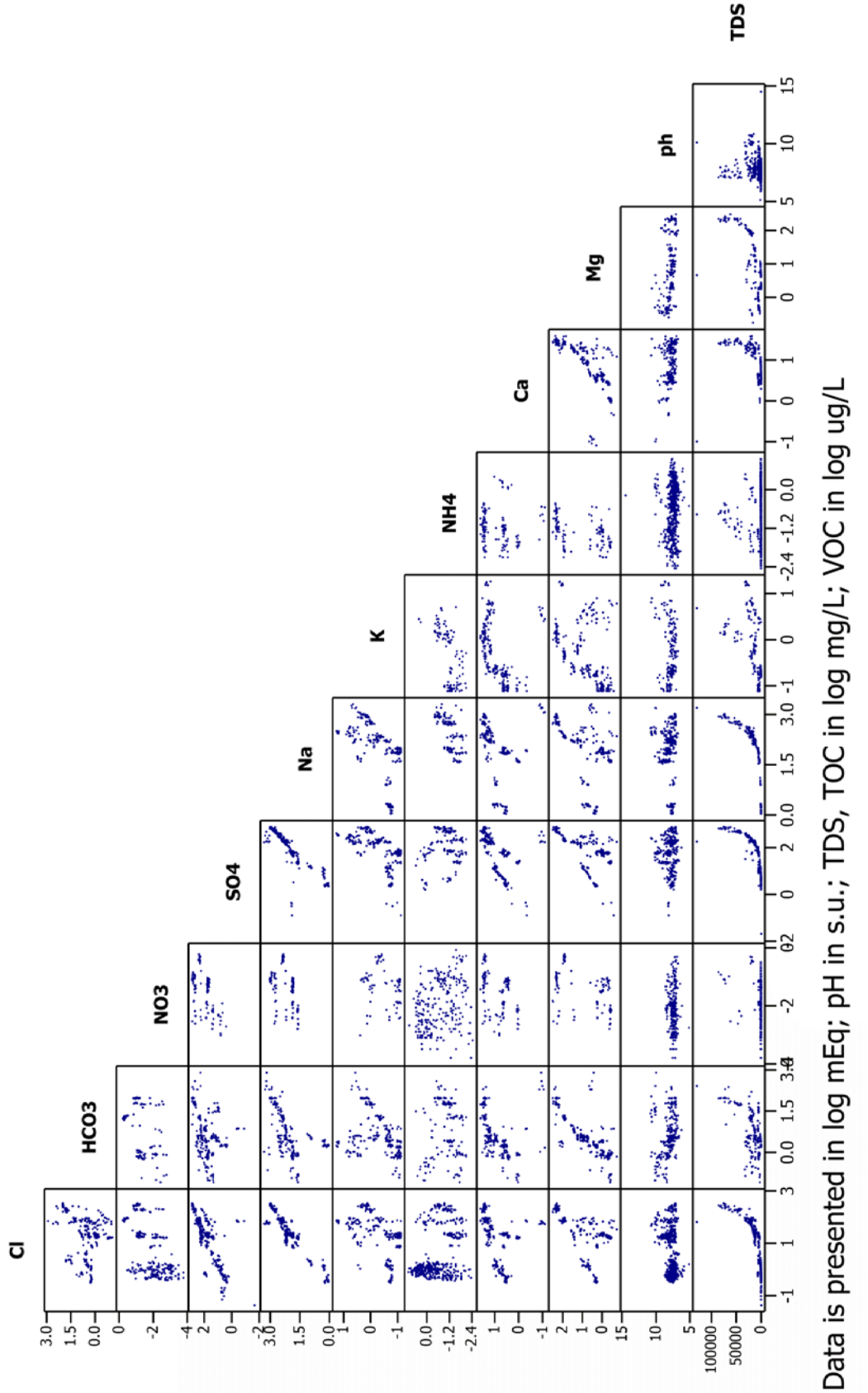
Industrial Landfill Data
Cl
HCO3
NO3
SO4
Na
K
NH4
Ca
Mg
ph
TDS
Data is presented in log mEq; pH in s.u.; TDS, TOC in log mg/L; VOC in log ug/L

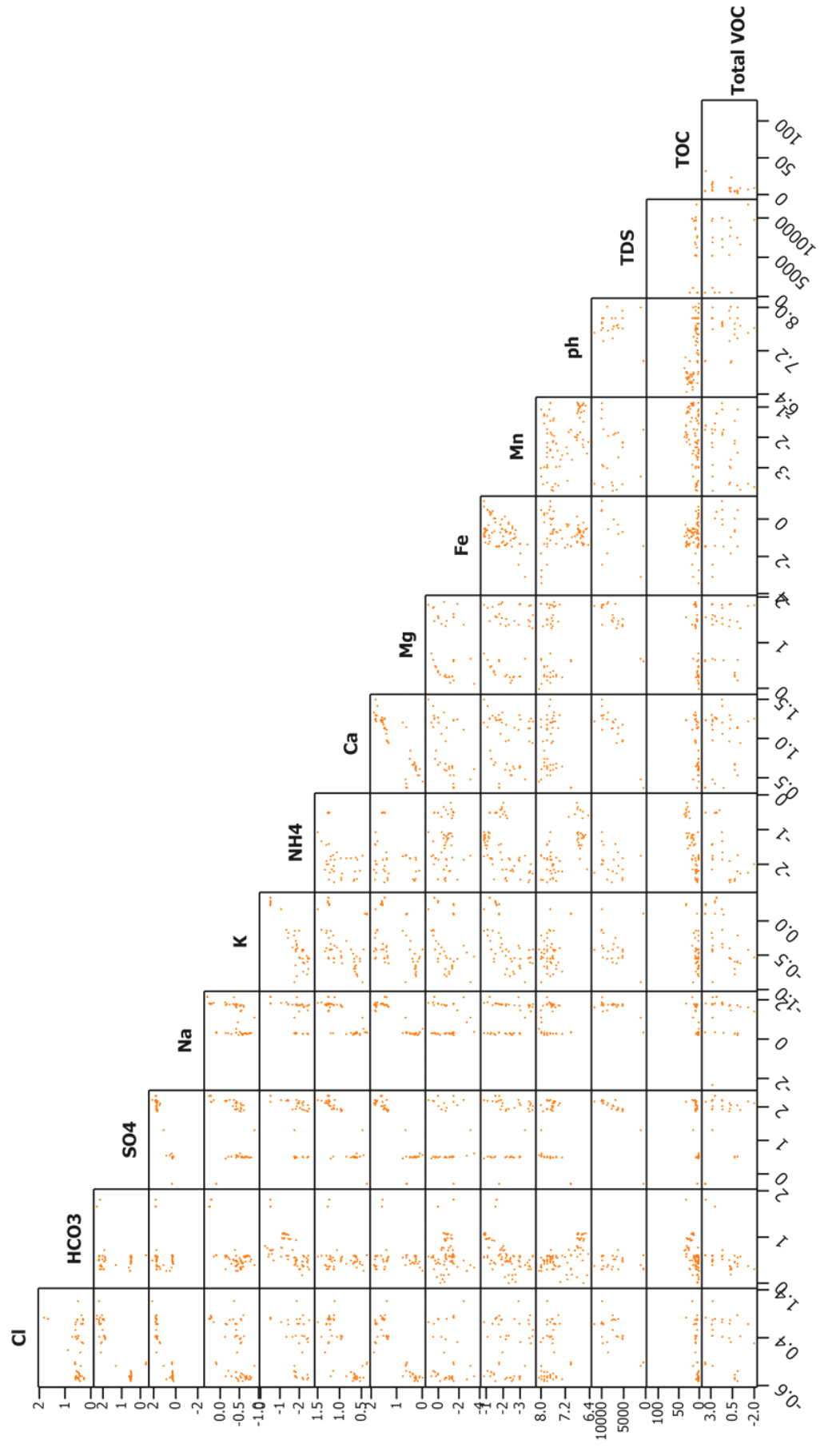

Data is presented in log mEq; pH in s.u.; TDS, TOC in log mg/L; VOC in log ug/L

Well	Model	Halite	Ion exchange	Illite	Thenardite	Calcite	CO2 gas	Dolomite	Na-Mont	Gypsum
R-9D	1	1.0456	20.25576	0.1153	-11.86331	3.58109	3.30668	2.17390	-2.13264	20.54073
	2	1.0456	-0.28497	0.1153	8.67742	3.63165	3.30668	0.35807	-2.13264	-
	5	1.0456	8.39245	0.1153	-	2.09746	3.30668	1.12517	-2.13264	8.67742
	7	1.0456	-	0.1153	8.39245	3.58127	3.30668	0.38327	-2.13264	0.28497
R-12	1	2.37595	-0.75782	0.15815	16.60428	-	0.42246	0.04024	-2.65074	2.08166
	5	2.37595	-1.86838	0.15815	17.71485	0.08048	0.42264	-	-2.65074	0.97109
R-18	1	0.36711	3.80878	0.11095	1.09102	-	0.71978	0.80869	-2.568	5.71459
	2	0.36711	-1.90581	0.11095	6.80561	1.29892	0.71978	0.15923	-2.568	-
	5	0.36711	-	0.11095	4.89980	0.86573	0.71978	0.37582	-2.568	1.90581
R-20	1	0.48282	-9.98635	0.25322	49.265	0.44858	1.62768	0.01608	-24.50672	-
	2	0.48282	-8.44921	0.25322	47.72787	-	1.62768	.24037	-24.5056	1.53713

Netpath modeling results show multiple net geochemical reactions which reproduce the concentrated sodium-sulfate rich waters that calibrate with Sand Draw landfill $\delta^{13}C$ values. The results of Netpath modeling above are stoichiometric coefficients reported in mmol L^{-1} H_2O where negative values are precipitating out of solution and positive values are dissolving into solution. In some instances negative and positive values represent the direction of ion exchange.

References

Ahern, J., Collentine, M, and Cooke, S. 1981. Occurrence and characteristics of ground water in the Green River Basin and Overthrust Belt, Wyoming. University of Wyoming Water Resources Research Institute report to U.S. Environmental Protection Agency, Vol. V-A and V-B: 123.

Appelo, C. A. J., and Postma, D. 1993. Geochemsitry, groundwater and pollution, Rotterdam, Netherlands: A. A. Balkema.

Back, W., Hanshaw, B. B., Plummer, L. N., Rahn, P. H., Rightmire, C. T. and Rubin, M. 1983. Process and rate of dedolomitization: Mass transfer and ^{14}C dating in a regional carbonate aquifer. Geological Society of America Bulletin, 94: 1415-1429.

Baedecker, M. J. and Back, W. 1979. Modern marine sediments as a natural analog to the chemically stressed environments of a landfill. Journal of Hydrology, 43: 393-414.

Benjamin, L., Knobel, L. L., Hall, L. F., Cecil, L. D., and Green, J. R. 2004. Development of a local meteoric water line for southeastern Idaho, western Wyoming, and south-central Montana. Scientific Investigations Report 2004-5126, United States Geological Survey.

Berner, R. A. and Morse, J. W. 1974. Dissolution kinetics of calcium carbonate in sea water: IV. Theory of calcite dissolution. American Journal of Science, 274: 108-134.

Bradley, W.H. 1964. Geology of Green River Formation and associated Eocene rocks in southwestern Wyoming and adjacent parts of Colorado and Utah. U.S. Geological Survey Professional Paper 496-A: A1-A86.

Christensen, T. H., Kjeldsen, P., Bjerg, P. L, Jensen, D. L., Christensen, J. B., Baun, A., Albrechtsen, H., Heron, G. 2001. Biogeochemistry of landfill leachate plumes. Applied Geochemistry, 16 : 659-718.

Clarey, K. E., Bartos, T., Copeland, D., Hallberg, L. L., Clark, M. L., and Thompson, M. L. 2010. WWDC Green River Basin water plan II: Groundwater study level 1 (2007-2009). Wyoming State Geological Survey.

Clark, I., and P. Fritz. 1997. Environmental Isotopes in Hydrology, CRC Press, Boca Raton, FL, 1997.

Collentine, M., Libra, R., Feathers, K. R., and Hamden L. 1981. Occurrence and Characteristics of Ground Water in the Great Divide and Washakie Basins, Wyoming. University of Wyoming Water Resources Research Institute report to U.S. Environmental Protection Agency, Vol. VI-A and VI-B: 112.

Craig, H. (1961) Isotopic variations in meteoric waters. Science, 133: 1702-1703.

Denson, N.M., and Pipiringos, G.N. 1974. Geologic map and sections showing areal distribution of Tertiary rocks near the southeastern terminus of the Wind River Range, Fremont and Sweetwater Counties, Wyoming, U.S. Geological Survey Miscellaneous Investigations Map I-835, scale 1:48,000.

Driscoll, D. G., Carter, J. M., Williamson, J. E, and Putnam, L. D. 2002. Table 4. Water-quality criteria, standards, or recommended limits for selected properties and constituents. Hydrology of the Black Hills Area, South Dakota: 46.

Environmental Protection Agency (EPA). 2012. Guide for industrial waste management. U.S. Environmental Protection Agency.

Environmental Protection Agency (EPA). 2007. SW-846: Test methods for evaluating solid wastes, physical/chemical methods, 6, U. S. Environmental Protection Agency.

Fan, M., DeCelles, P. G., Gehrels, G. E., Dettman, D. L., Quade, J., and Peyton, S. L. 2011. Sedimentology, detrital zircon geochronology, and stable isotope geochemistry of the lower Eocene strata in the Wind River Basin, central Wyoming, Geological Society of America Bulletin, 123, 5: 979-996.

Feathers, K. R., Libra, R., and Stephenson, T. R. 1980. Occurrence and Characteristics of Ground Water in the Powder River Basin, Wyoming, University of Wyoming Water Resources Research Institute report to U.S. Environmental Protection Agency, Vol. I-A and I-B (1981): 203.

Freeze, A. and Cherry, J. A. 1979. Groundwater. New Jersey: Prentice-Hall, Inc.

Gibb, J. P., Schuller, R. M., and Griffin, R. A. 1981. Procedures for the collection of representative water quality data from monitoring wells. Cooperative Resources Report.

Gill, J.R., Merewether, E.A., and Cobban, W.A. 1970. Stratigraphy and nomenclature of some Upper Cretaceous and lower Tertiary rocks in south-central Wyoming. U.S. Geological Survey Professional Paper 667: 53.

Gill, J.R., and Cobban, W.A. 1973. Stratigraphy and geologic history of the Montana Group and equivalent rocks, Montana, Wyoming, and North and South Dakota, U.S. Geological Survey Professional Paper 776: 37.

Green, G. N. and Drouillard, P. H. 1994. The digital geologic map of Wyoming in ARC/INFO format: U.S. Geological Survey Open-File Report 94-0425.

Gurdak, J. J. and Roe, C. D. 2010. Review: Recharge rates and chemistry beneath playas of the High Plains aquifer, USA. Hydrogeology Journal, 18: 1747-1772.

Hem, J. D. 1985. Study and interpretation of the chemical characteristics of natural water. U.S Geological Survey Water-Supply Paper 2254, 3.

Hidalgo, M. C. and Cruz-Sanjulián, J. 2001. Groundwater composition, hydrochemical evolution and mass transfer in a regional detrital aquifer (Baza basin, southern Spain), Applied Geochemistry, 16: 745-758.

Jin, L. and Siegel, D. I. 2008. Temporal geochemical variations in a mountain stream: expectations to anomalies, Abstract, AGU Fall Meeting, San Francisco, CA.

Jin, L. 2008. Evaluating spatial and temporal variations of water chemistry and the impact of transient storage on solute transport in low-order mountain streams. PhD Dissertation, Syracuse University.

Jin, L., Siegel, D. I., Lautz, L. K., Mitchell, M. J., Dahms, D. E., and Mayer, B. 2009. Calcite precipitation driven by the common isotope effect during groundwater-surface-water mixing: A potentially common process in streams with geologic settings containing gypsum, Geological Society of America.

Keefer, W.R. 1965. Stratigraphy and geologic history of the uppermost Cretaceous, Paleocene, and lower Eocene rocks in the Wind River Basin, Wyoming. U.S. Geological Survey Professional Paper 495-A: 77.

Keefer, W. R. 1970. Structural geology of the Wind River Basin, Wyoming. U.S. Geological Survey Professional Paper 495-D: 35.

Keefer, W. R. 1972. Frontier, Cody, and Mesaverde Formations in the Wind River and southern Bighorn Basins, Wyoming. U.S. Geological Survey Professional Paper 495-E: 23.

Keefer, W.R., and Van Lieu, J.A. 1966. Paleozoic formations in the Wind River Basin, Wyoming. U.S. Geological Survey Professional Paper 495-B: 60.

Kendall, C., and Coplen, T. B. 2001. Distribution of oxygen-18 and deuterium in river waters across the United States, Hydrologic Processes, 15: 1363-1393.

Libra, Robert D., Collentine, M., and Feathers, K. R. 1981a. Occurrence and Characteristics of Ground Water in the Denver-Julesburg Basin, Wyoming, University of Wyoming Water Resources Research Institute report to U.S. Environmental Protection Agency, Vol. VII-A and VII-B: 101.

Libra, R., Doremus, D., and Goodwin, C. 1981b. Occurrence and Characteristics of Ground Water in the Bighorn Basin, Wyoming, University of Wyoming Water Resources Research Institute report to U.S. Environmental Protection Agency, Vol. II-A and II-B: 104.

Love, J.D., and Christiansen, A.C. 1980. Preliminary correlation of stratigraphic units used on 1° x 2° geologic quadrangle maps of Wyoming, in Stratigraphy of Wyoming. Wyoming Geological Association 31st Annual Field Conference Guidebook: 279-282.

Love, J. D. and Christiansen, A. C. 1985. Geologic map of Wyoming, U. S. Geological Survey.

Love, J.D., Christiansen, A.C., Bown, T.M., and Earle, J.L., compilers. 1979. Preliminary geologic map of the Thermopolis 1° x 2° Quadrangle, central Wyoming. U.S. Geological Survey Open-File Report 79-962, scale 1:250,000.

Love, J.D., Christiansen, A.C., and Earle, J.L., compilers. 1978a. Preliminary geologic map of the Sheridan 1° x 2° Quadrangle, northern Wyoming. U.S. Geological Survey OpenFile Report 78-456, scale 1:250,000.

Love, J.D., Christiansen, A.C., Earle, J.L., and Jones, R.W., compilers. 1978b. Preliminary geologic map of the Arminto 1° x 2° Quadrangle, central Wyoming. U.S. Geological Survey Open-File Report 78-1089, scale 1:250,000.

Love, J.D., Christiansen, A.C., Earle, J.L., and Jones, R.W., compilers. 1979a. Preliminary geologic map of the Casper 1° x 2° Quadrangle, central Wyoming. U.S. Geological Survey Open-File Report 79-961, scale 1:250,000.

Love, J.D., Christiansen, A.C., and Jones, R.W., compilers. 1979b. Preliminary geologic map of the Lander 1° x 2° Quadrangle, central Wyoming. U.S. Geological Survey Open-File Report 79-1301, scale 1:250,000.

Love, J.D., Christiansen, A.C., McGrew, L.W., and King, Jon, compilers. 1990. Geologic map of the Gillette 1° x 2° Quadrangle, northeastern Wyoming and western South Dakota. Geological Survey of Wyoming Map Series 25I, scale 1:250,000.

Love, J.D., Christiansen, A.C., and Sever, C.K., compilers. 1980. Geologic map of the Torrington 1° x 2° Quadrangle, southeastern Wyoming and western Nebraska. U.S. Geological Survey Miscellaneous Field Studies Map MF-1184, scale 1:250,000.

Mapel, W. J., and Pillmore, C. L. 1963. Geology of the Newcastle Area, Weston County Wyoming. Contributions to General Geology, Geological Survey Bulletin 1141-N.

Maughan, E.K. 1964. The Goose Egg Formation in the Laramie Range and adjacent parts of southeastern Wyoming, U.S. Geological Survey Professional Paper 501-B: B53-B60.

McGrew, L.W. 1963. Geology of the Fort Laramie area, Platte and Goshen Counties, Wyoming, U.S. Geological Survey Bulletin 1141-F: 39.

Miller, D. M., Nilsen, T. H., and Bilodeau, W. L. 1992. Late Cretaceous to early Eocene geologic evolution of the U.S. Cordillera. The Geology of North America: The Cordilleran Orogen, Conterminous U.S., G-3: 205-260.

Motzer, W. E, Mohr, T. K. G, McCraven, S. and Stanin, P. 2006. Stable and other isotope techniques for perchlorate source identification. Environmental Forensics, 7:1, 89-100.

Nativ, R., Adar, E., Dahan, O., and Nissim, I. 1997. Water salinization in arid regions – observations from the Negev desert, Israel. Journal of Hydrology, 196: 271-296.

Neasham, J. W. and Vondra, C. F. 1972. Stratigraphy and petrology of the Lower Eocene Willwood Formation, Bighorn Basin, Wyoming. Geological Society of America Bulletin, 83, 7: 2167-2180.

Ong, C. G, Tanji, K. K., Dahlgren, R. A., Smith, G. R., and Quek, A. F. 1995. Water quality and trace element evapoconcentration in evaporation ponds for agricultural waste water disposal, Journal of Agricultural and Food Chemistry, 43, 7: 1941-1947.

Oriel, S.S., and Platt, L.B. 1980. Geologic map of the Preston 1° x 2° Quadrangle, southeastern Idaho and western Wyoming, U. S. Geological Survey Miscellaneous Investigations Map I-1127; scale 1:250,000.

Person, M., McIntosh, J., Bense, V., and Remenda V. H. 2007. Pleistocene hydrology of North America: The role of ice sheets in reorganizing groundwater flow systems. Reviews of Geophysics: 45.

Plummer, L. N. and Back W. 1980. The mass balance approach: Application to interpreting the chemical evolution of hydrologic systems, American Journal of Science, 280: 130-142.

Plummer, L. N., Parkhurst, D. L., and Thorstenson, D. C. 1983. Development of reaction models for ground-water systems. Cehcoemica et Cosmochimica Acta, 47, 4: 665-686.

Plummer, L. N., Prestemon, E. C., and Parkhurst, D. L. 1994. An interactive code (NETPATH) for modeling net geochemical reactions along a flow path: Version 2.0. Water-Resources Investigations Report 94-4169, United States Geological Survey.

Plummer, L. N. and Sprinkle, C. L. 2001. Radiocarbon dating of dissolved inorganic carbon in groundwater from confined parts of the Upper Floridan aquifer, Florida, USA. Hydrogeology Journal, 9: 127-150.

Pokrovsky, O. S. and Schott, J. 2001. Kinetics and mechanism of dolomite dissolution in neutral to alkaline solutions revisited, American Journal of Science, 301: 597-626.

Richter, H. R. 1981a. Occurrence and Characteristics of Ground Water in the Wind River Basin, Wyoming, University of Wyoming Water Resources Research Institute report to U.S. Environmental Protection Agency, Vol. IV-A and IV-B: 149.

Richter, H. R., 1981b, Occurrence and Characteristics of Ground Water in the Laramie, Shirley, and Hanna Basins, Wyoming. University of Wyoming Water Resources Research Institute report to U.S. Environmental Protection Agency, Vol. III-A and III-B: 117.

Roehloer, H. W. 1991. Revised stratigraphic nomenclature for the Wasatch and Green River Formations, in Geology of the Eocene Wasatch, Green River, and Bridger (Washakie) Formations, Green River Basin, Wyoming, Utah, and Colorado. U.S. Geological Survey Professional Paper 1506-B: 38.

Saar, R. A. 1997. Filtration of ground water samples: A review of industry practice. Groundwater Monitoring and Remediation: 56-62.

Sheldon, R. P. 1923. Physical stratigraphy of the phosphoria formation in northwestern Wyoming. Contributions to Economic Geology, Geological Survey Bulletin 1042-E.

Siegel, D. I. 2009. Compartmentalization of ground water at the Sand Draw #2 Landfill site: Assessing independent and multidisciplinary approaches. Fremont County Landfill Authority, September 28, 2009.

Siegel, D. I. 2011. Water levels, Sand Draw Landfill, 2011.

Siegel, D. I. 2011. Resistivity transect, Sand Draw Landfill 2011.

Siegel, D. I. 2011. Potentiometric surface: Sand Draw Landfill Fremont County, Wyoming, Trihydro operations, April 27, 2010.

Stillings, L. L, Drever, J. I., Brantley, S. L., Sun, Y., and Oxburgh, R. 1996. Rates of feldspar dissolution at pH 3-7 with 0-8 m M oxalic acid, Chemical Geology, 132: 79-89.

Taucher, P., Bartos, T. T., Clarey, K. E., Quillinan, S. A., Hallberg, L. L, Clark, M. L., Thompson, M., Gribb, N., Worman, B., and Gracias, T. 2012. Wind/Bighorn River Basin water plan update: Groundwater study level 1 (2008-2011), Wyoming State Geological Survey, Laramie, Wyoming.

United States Environmental Protection Agency. 2009. National Primary Drinking Water Regulations.

Wyoming Wellhead Protection Strategy Committee (WWPSC). 1997. Wyoming State Wellhead Protection Guidance Document. Cheyenne, WY.

Wyoming Department of Environmental Quality. 1995. Solid waste guideline #15: Groundwater sampling procedures, Solid waste and Hazardous Waste Division, October 25, 1995.

Wyoming Department of Environmental Quality. 2007. Quality standards for Wyoming groundwaters, Water Quality Rules and Regulations, 9.

Wyoming Department of Environmental Quality. 2010. Groundwater impacts and remediation costs: Wyoming municipal solid waste disposal facilities, Joint Miner., Business, and Econ. Dev. Interim Comm., Wyoming, 30 July.

Wyoming Department of Environmental Quality. 2013. Groundwater sampling and analysis requirements, Solid Waste Rules and Regulations, 2: 2-47.

Wyoming State Geological Survey (WSGS). 2014. Wyoming stratigraphy index map.

Vita

Name of Author: Maxwell Blaine Gade

Place of Birth: Lincoln, Nebraska

Date of Birth: June 18, 1989

Undergraduate School Attended:

- University of Nebraska, Lincoln, Nebraska